2

ELECTRICAL ENGINEERING

N71-17445 (ACCESSION NUMBER)
G3 (THRU)
77 (PAGES)
(CODE)
CR-103026 (NASA CR OR TMX OR AD NUMBER)
21 (CATEGORY)
FACILITY FORM 602

ENGINEERING EXPERIMENT STATION
AUBURN UNIVERSITY
AUBURN, ALABAMA

Reproduced by
NATIONAL TECHNICAL
INFORMATION SERVICE
Springfield, Va. 22151

STUDY OF AN IMPROVED ATTITUDE

CONTROL SYSTEM

PREPARED BY

GUIDANCE AND CONTROL STUDY GROUP

JOSEPH S. BOLAND, III, PROJECT LEADER

TWENTY FIFTH TECHNICAL REPORT

DECEMBER 14, 1970

CONTRACT NAS8-20104
GEORGE C. MARSHALL SPACE FLIGHT CENTER
NATIONAL AERONAUTICS AND SPACE ADMINISTRATION
HUNTSVILLE, ALABAMA

APPROVED BY:

Chester C. Carroll

Chester C. Carroll
Professor and Head
Electrical Engineering

SUBMITTED BY:

Joseph S. Boland, III

Joseph S. Boland, III
Assistant Professor
Electrical Engineering

TABLE OF CONTENTS

FOREWORD

This report is a technical summary of the progress made by the Electrical Engineering Department, Auburn University, toward fulfillment of Contract NAS8-20104 granted to Auburn Research Foundation, Auburn, Alabama. This contract was awarded April 6, 1965, by the George C. Marshall Space Flight Center, National Aeronautics and Space Administration, Huntsville, Alabama.

SUMMARY

The investigation of an Improved Attitude Control System for an orbiting space vehicle is presented in this report. A steering law is developed which greatly reduces the cross-axis responses of the system. The system stability is shown not to be adversely affected.

PERSONNEL

The following staff members of Auburn University are active participants in the work of this contract:

J. S. Boland, III - Assistant Professor of Electrical Engineering

Brij Bhushan - Graduate Research Assistant, Electrical Engineering

Michael H. Fong - Graduate Research Assistant, Electrical Engineering

D. W. Sutherlin - Graduate Research Assistant, Electrical Engineering

LIST OF FIGURES

LIST OF TABLES

LIST OF SYMBOLS

SYMBOL	DEFINITION
i, j	General subscripts (range 1, 2, 3)
$\overline{}$	Bar above a letter indicates a vector quantity
C	Cosine
G_1, G_3	Compensation networks for the inner and outer gimbal velocity servos, respectively
$G_{cc(1)}$, $G_{cc(3)}$	Crossfeed compensation for the inner and outer gimbal velocity servos, respectively
H	Magnitude of the momentum of the CMG's
$\overline{H}_T$	Total momentum vector of the CMG's
$\overline{H}_c$	Time integral of the attitude control system moment command
$\overline{H}_E$	Error signal between $\overline{H}_c$ and $\overline{H}_T$
[I]	Identity Matrix
J_1	$= J_{11} - Ng(1 + Ng)\ J_{MR}$
J_3	$= -\frac{1}{2} \text{Sin}\ 2\delta_1 [(J_{A33} + J_D) - (J_{A22} + J_D)]$
J_{11}	$= N_g^2\ J_{MR} + J_{A11} + J_D$
J_{33}	$= N_g^2\ J_{MR} + J_{C33} + (J_{A33} + J_D)\ \text{Cos}^2\delta_1 + (J_{A22} + J_R)\text{Sin}^2\delta_1$
J_R	$\equiv$ Polar moment of inertia of the CMG wheel about the $\overline{1}_{2A}$ vector
J_D	$\equiv$ Polar moment of inertia of the wheel about an axis perpendicular to the $\overline{1}_{2A}$ vector

SYMBOL	DEFINITION
J_{A11}, J_{A22}, J_{A33}	≡ Polar moment of inertia of the inner gimbal exclusive of the wheel about the $\bar{1}_{1A}$, $\bar{1}_{2A}$ $\bar{1}_{3A}$ vectors, respectively.
J_{C33}	Polar moment of inertia of the outer gimbal about the $\bar{1}_{3C}$ vector.
J_{MR}	≡ Polar moment of inertia of the torque motor rotor about its rotational axis
K_{SL}	Gain Constant
M_R	Reaction moment of the CMG's on the base of the vehicle
N_g	Gear ratio of the gimbal drives
s	Laplace operator
S	Sine
$[T_s]$	Steering Law
$\delta_{1(j)}$	Inner gimbal angle of the j^{th} CMG
$\delta_{3(j)}$	Outer gimbal angle of the j^{th} CMG
$\dot{\delta}_{1(j)}$, $\dot{\delta}_{3(j)}$	Time rate of change of angles $\delta_{1(j)}$, $\delta_{3(j)}$
$\bar{\omega}_{VA(j)}$	Inner gimbal rate of the j^{th} CMG with respect to vehicle space

I. INTRODUCTION

One of the primary objectives of the Apollo Telescope Mount (ATM) Mission is to increase the knowledge of the solar environment. The ATM is a manned solar observatory from which solar data may be acquired and solar experiments performed. With the ATM in earth orbit, the experimenter is free to perform experiments in an essentially atmosphere-free environment. The basic configuration includes an Apollo service and command module, an S-IVB workshop, a multiple docking adapter, and the ATM rack as shown in Figure 1.[1]

The desired experiment conditions necessitate highly accurate pointing requirements. These pointing requirements must be maintained by the control system when the system is under the influence of both external and internal torques such as gravity gradient and aerodynamic torques or astronaut motion.

For the pointing control subsystem, roll is defined as the angular rotation about the line-of-sight from the ATM rack to the center of the sun with pitch and yaw being the small deviations of the ATM rack with respect to this line of sight.

The Control Moment Gyro (CMG) control system for the ATM rack was chosen principally because of performance benefits with regard to the effective compensation of cyclic disturbance torques such as gravity gradient and aerodynamic torques and with regard to the dynamic

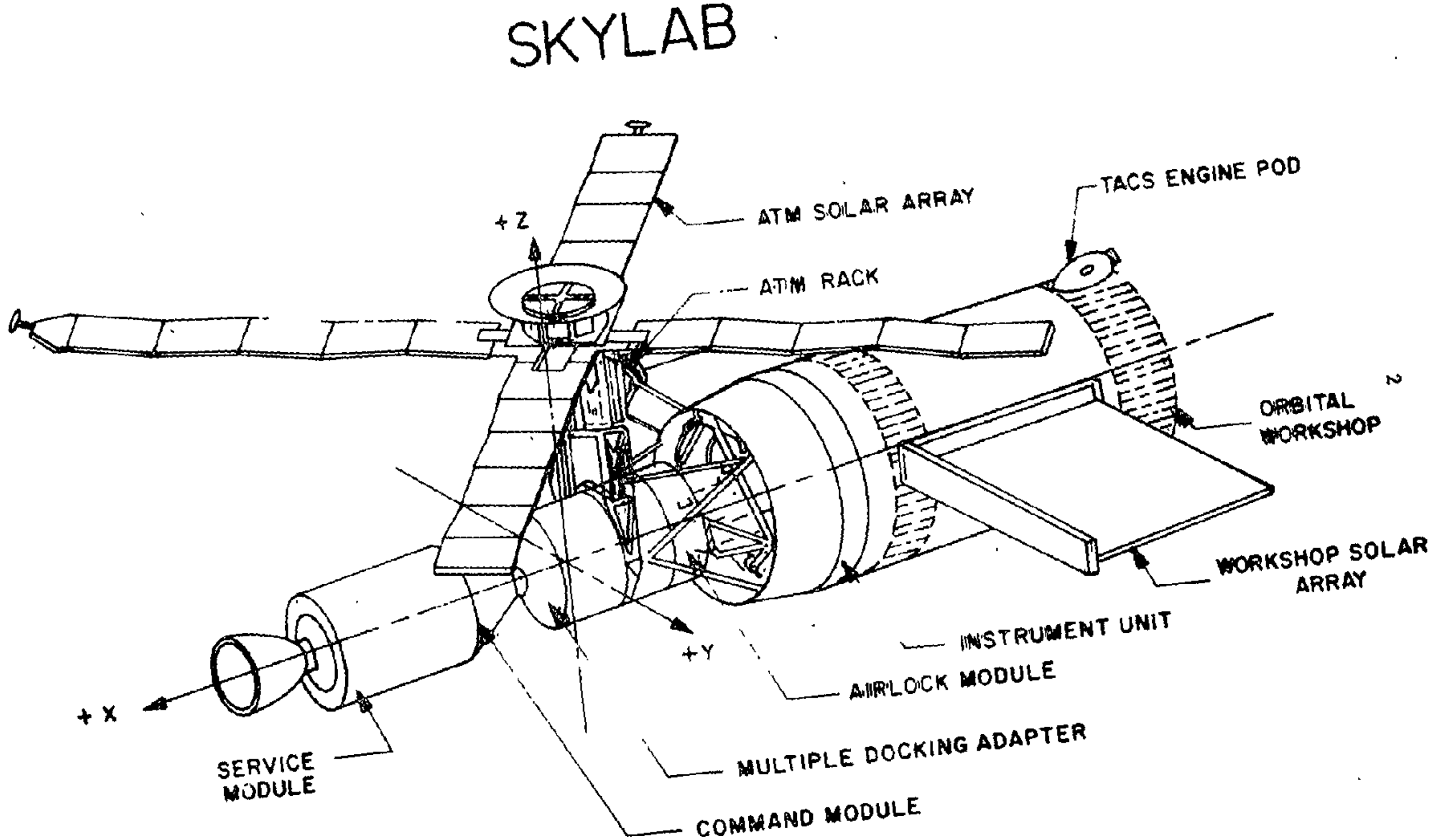

Figure 1. Basic Skylab Configuration.

characteristics of the system. A passive control system (gravity gradient, for example) would not, in general, have the required accuracy and would not develop sufficient torques to meet the dynamic performance requirements. Also during periods when the experiment optics are exposed, use of the CMG pointing control subsystem prevents possible optics contamination that could occur from the exhaust of a reaction jet control system. However, the reaction jet control system of the Lunar Excursion Module could be utilized for a coarse control system and could also be available for use in CMG momentum desaturation.

The CMG is basically a gimbaled wheel rotating at a constant speed which provides a constant angular momentum and is capable of having a variable orientation with respect to the spacecraft. A moment is imparted to the vehicle by causing a change in the direction of the constant momentum.

Two of the primary design requirements of the attitude control system for the Apollo Telescope Mount are; (1) the minimization of the cross-axis response and, (2) the maximization of the direct-axis bandwidth.

II. DERIVATION OF REACTION MOMENT EQUATIONS

The CMG is a two degree of freedom gyroscopic device as shown schematically in Figure 2. It consists of a constant speed wheel held in a housing referred to as the inner gimbal. The inner gimbal is coupled to the outer gimbal by the pivot designated as (1). The (1) pivot is perpendicular to the momentum vector of the wheel. The pivot designated as (3) couples the outer gimbal to the base of the CMG. The (3) pivot is perpendicular to the (1) pivot.

There are 3 spaces which will be used in the derivation of the reaction moment equations of the CMG. These are shown in Figure 2 and are

1. Inner gimbal space, A-space, designated by $\bar{1}_{1A}$, $\bar{1}_{2A}$, and $\bar{1}_{3A}$.
2. Outer gimbal space, C-space, designated by $\bar{1}_{1C}$, $\bar{1}_{2C}$, and $\bar{1}_{3C}$.
3. Base space of the CMG, B-space, designated by $\bar{1}_{1B}$, $\bar{1}_{2B}$ and $\bar{1}_{3B}$.

The CMG cluster showing the mounting planes and the positive directions for the gimbal angles is shown in Figure 3. The reaction moment of a cluster of ideal CMG's can be expressed in inertial space as:

$$\bar{M}_{RV} = - \left. \frac{d\bar{H}}{dt} \right|_{\text{I-space}}$$

where an ideal CMG is defined as having instantaneous control loops

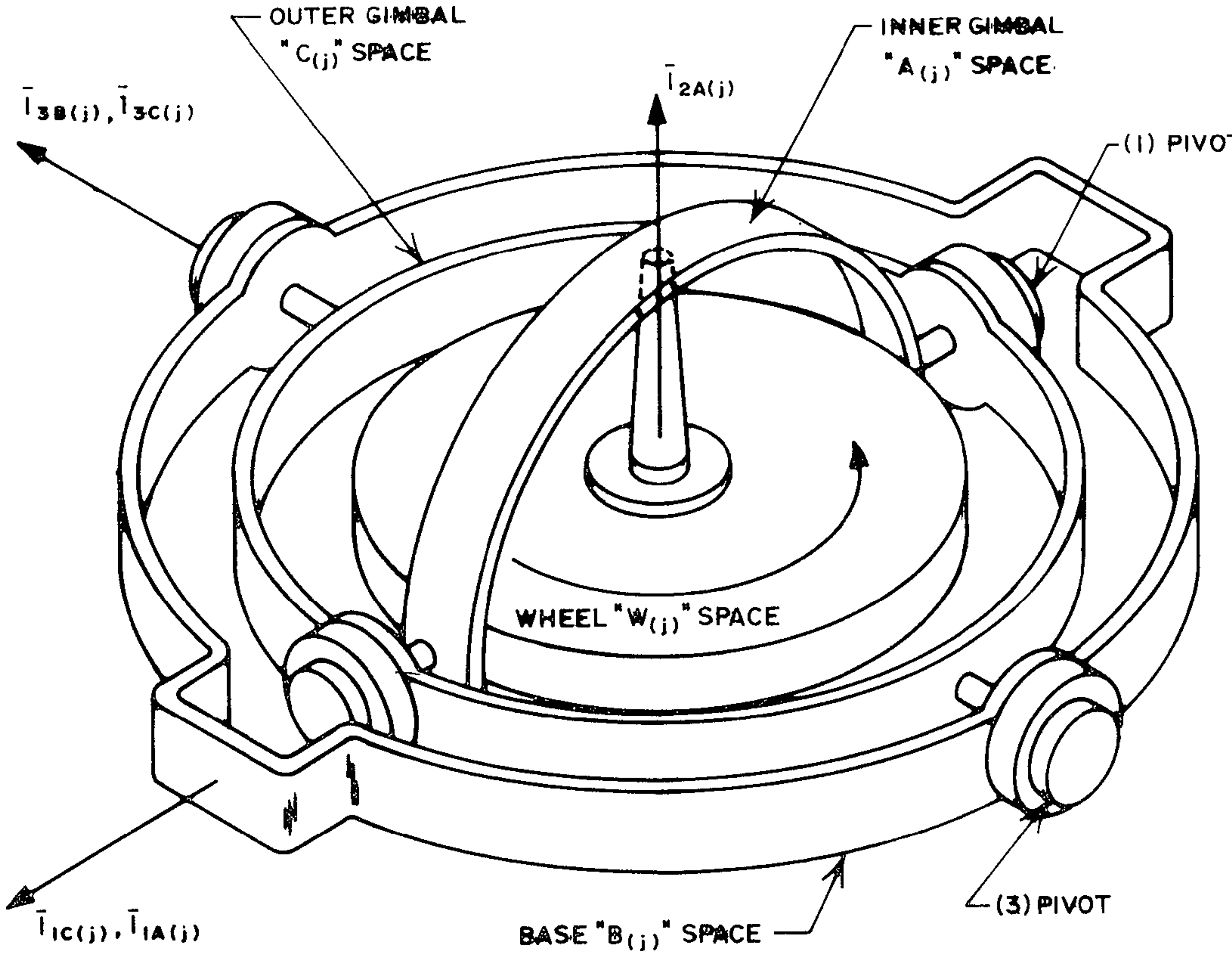

Figure 2. Schematic of j^{th} CMG.

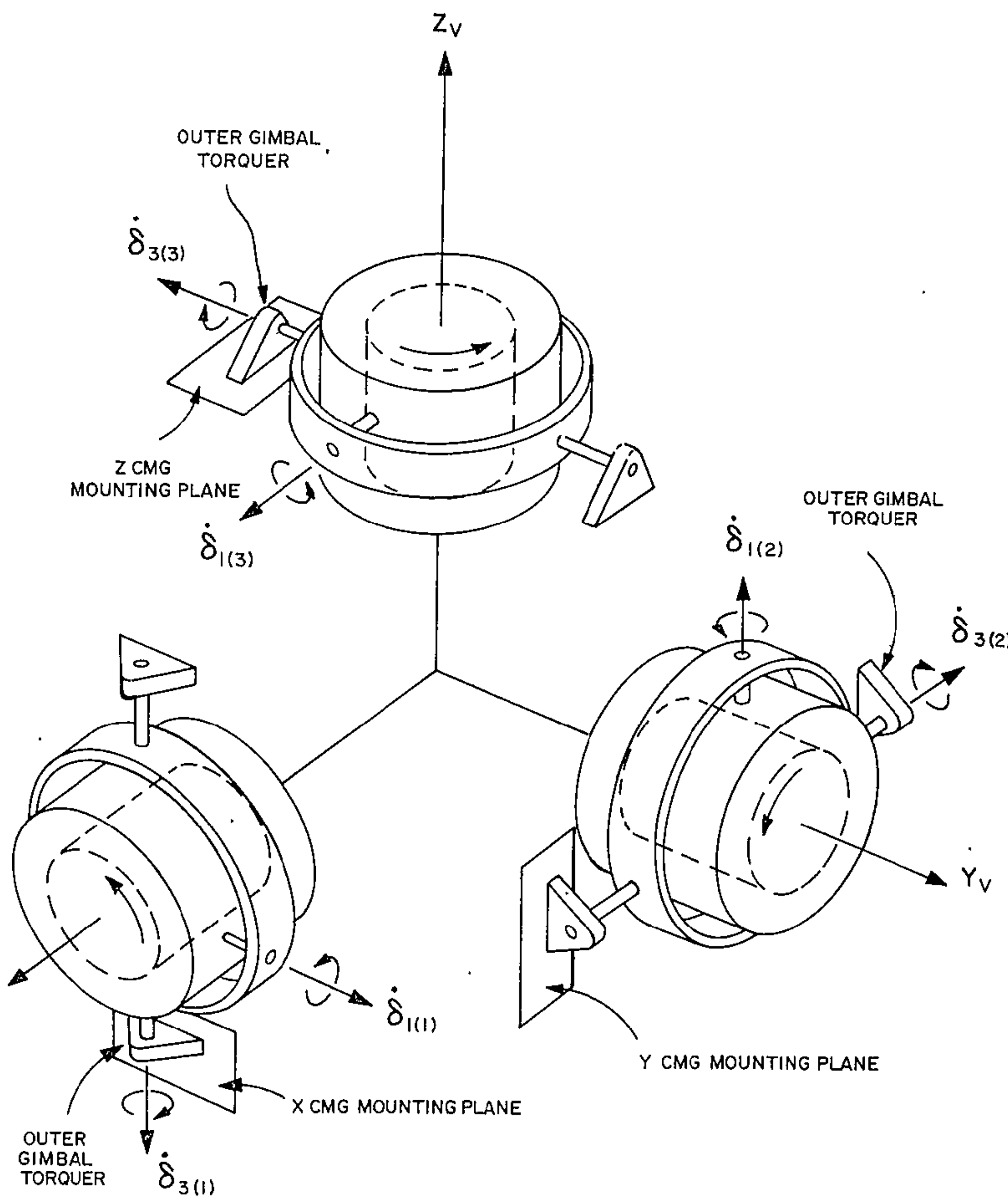

Figure 3. CMG Cluster

and no inertia reaction moments. This may be written, in vehicle space, as

$$\overline{M}_{RV} = - \frac{d\overline{H}_V}{dt_V} + \omega_{IV} \times \overline{H}$$

In A-space, the reaction moment may be expressed as:

$$\overline{M}_{RV} = - \sum_{j=1}^{3} \frac{dH_{A(j)}}{dt_A} + \overline{\omega}_{VA} \times \overline{H}_{A(j)} + \omega_{IV} \times \overline{H}_V$$

The inertial velocity, ω_{IV} is nominally zero. The wheel speed is a constant so that

$$\frac{dH_A}{dt_A} = 0$$

Thus, the expression for the reaction moment may be written as:

$$\overline{M}_{RV} = - \sum_{j=1}^{3} \overline{\omega}_{VA(j)} \times \overline{H}_{A(j)}$$

The transformation matrix from A to C space is

$$\begin{bmatrix} H_{1C(j)} \\ H_{2C(j)} \\ H_{3C(j)} \end{bmatrix} = \begin{bmatrix} 1 & 0 & 0 \\ 0 & C_{\delta 1(j)} & -S_{\delta 1(j)} \\ 0 & S_{\delta 1(j)} & C_{\delta 1(j)} \end{bmatrix} \begin{bmatrix} H_{1A(j)} \\ H_{2A(j)} \\ H_{3A(j)} \end{bmatrix} = [A] \begin{bmatrix} H_{1A(j)} \\ H_{2A(j)} \\ H_{3A(j)} \end{bmatrix}$$

where C's and S's represent cosine and sine terms, respectively. The transformation matrix from C to B space is

$$\begin{bmatrix} H_{1B(j)} \\ H_{2B(j)} \\ H_{3B(j)} \end{bmatrix} = \begin{bmatrix} C_{\delta 3(j)} & -S_{\delta 3(j)} & 0 \\ S_{\delta 3(j)} & C_{\delta 3(j)} & 0 \\ 0 & 0 & 1 \end{bmatrix} \begin{bmatrix} H_{1C(j)} \\ H_{2C(j)} \\ H_{3C(j)} \end{bmatrix} = [B] \begin{bmatrix} H_{1C(j)} \\ H_{2C(j)} \\ H_{3C(j)} \end{bmatrix}$$

The transformation from A to B space is then:

$$\begin{bmatrix} H_{1B(j)} \\ H_{2B(j)} \\ H_{3B(j)} \end{bmatrix} = [B]\ [A] \begin{bmatrix} H_{1A(j)} \\ H_{2A(j)} \\ H_{3A(j)} \end{bmatrix}$$

where

$$[B]\ [A] = \begin{bmatrix} C_{\delta 3(j)} & -S_{\delta 3(j)} C_{\delta 1(j)} & S_{\delta 3(j)} S_{\delta 1(j)} \\ S_{\delta 3(j)} & C_{\delta 3(j)} C_{\delta 1(j)} & -C_{\delta 3(j)} S_{\delta 1(j)} \\ 0 & S_{\delta 1(j)} & C_{\delta 1(j)} \end{bmatrix}$$

Also,

$$\overline{H}_{A(j)} = \overline{1}_{2A(j)}\ H_{(j)}.$$

With this relationship, the reaction moment applied by the j^{th} CMG on its base may be expressed as:

$$\begin{bmatrix} M_{R1B(j)} \\ M_{R2B(j)} \\ M_{R3B(j)} \end{bmatrix} = H(j) \begin{bmatrix} -S_{\delta 3(j)} S_{\delta 1(j)} & 0 & C_{\delta 1(j)} C_{\delta 3(j)} \\ C_{\delta 3(j)} S_{\delta 1(j)} & 0 & C_{\delta 1(j)} S_{\delta 3(j)} \\ -C_{\delta 1(j)} & 0 & 0 \end{bmatrix} \begin{bmatrix} \dot{\delta}1(j) \\ 0 \\ \dot{\delta}3(j) \end{bmatrix}$$

From Figure 3, the relationship between the reaction moment in base space to vehicle space is as follows:

#1 CMG

$$\begin{bmatrix} M_{RXV} \\ M_{RYV} \\ M_{RZV} \end{bmatrix} = \begin{bmatrix} 0 & 1 & 0 \\ 1 & 0 & 0 \\ 0 & 0 & -1 \end{bmatrix} \cdot \begin{bmatrix} M_{R1B} \\ M_{R2B} \\ M_{R3B} \end{bmatrix}$$

#2 CMG

$$\begin{bmatrix} M_{RXV} \\ M_{RYV} \\ M_{RZV} \end{bmatrix} = \begin{bmatrix} 0 & 0 & -1 \\ 0 & 1 & 0 \\ 1 & 0 & 0 \end{bmatrix} \begin{bmatrix} M_{R1B} \\ M_{R2B} \\ M_{R3B} \end{bmatrix}$$

#3 CMG

$$\begin{bmatrix} M_{RXV} \\ M_{RYV} \\ M_{RZV} \end{bmatrix} = \begin{bmatrix} 1 & 0 & 0 \\ 0 & 0 & -1 \\ 0 & 1 & 0 \end{bmatrix} \begin{bmatrix} M_{R1B} \\ M_{R2B} \\ M_{R3B} \end{bmatrix}$$

From these relationships, the reaction moment of the cluster on the vehicle may be determined as:

$$M_{RXV} = M_{R2B(1)} - M_{R3B(2)} + M_{R1B(3)}$$

$$M_{RYV} = M_{R1B(1)} + M_{R2B(2)} - M_{R3B(3)}$$

$$M_{RZV} = -M_{R3B(1)} + M_{R1B(2)} + M_{R2B(3)}$$

Expanding and collecting terms, the relationship between the reaction moments and the gimbal rates may be written as

$$\begin{bmatrix} M_{RXV} \\ M_{RYV} \\ M_{RZV} \end{bmatrix} = [A] \, [\dot{\delta}_{1(1)} \quad \dot{\delta}_{1(2)} \quad \dot{\delta}_{1(3)} \quad \dot{\delta}_{3(1)} \quad \dot{\delta}_{3(2)} \quad \dot{\delta}_{3(3)}]^T$$

where $[\ ]^T$ denotes the transpose and [A] is given by

$$\begin{bmatrix} C_{\delta 3(1)} S_{\delta 1(1)} & C_{\delta 1(2)} & -S_{\delta 3(3)} S_{\delta 1(3)} & C_{\delta 1(1)} S_{\delta 3(1)} & 0 & C_{\delta 1(3)} C_{\delta 3(3)} \\ -S_{\delta 3(1)} S_{\delta 1(1)} & C_{\delta 3(2)} S_{\delta 1(2)} & C_{\delta 1(3)} & C_{\delta 1(1)} C_{\delta 3(1)} & C_{\delta 1(2)} S_{\delta 3(2)} & 0 \\ C_{\delta 1(1)} & -S_{\delta 3(2)} S_{\delta 1(2)} & C_{\delta 3(3)} S_{\delta 1(3)} & 0 & C_{\delta 1(2)} C_{\delta 3(2)} & C_{\delta 1(3)} S_{\delta 3(3)} \end{bmatrix}$$

The six CMG gimbal rates are commanded based on information obtained from body mounted sensors. This three-dimensional information must then be used to provide the gimbal rates which provide the desired reaction moment to counteract the disturbance moment. The transformation that gives this six-dimensional command vector from the three-dimensional sensed information is called the steering law. In equation form, this may be written as:

$$\begin{bmatrix} \dot{\delta}_{1(1)C} \\ \dot{\delta}_{1(2)C} \\ \dot{\delta}_{1(3)C} \\ \dot{\delta}_{3(1)C} \\ \dot{\delta}_{3(2)C} \\ \dot{\delta}_{3(3)C} \end{bmatrix} = [T_S] \begin{bmatrix} M_{CXV} \\ M_{CYV} \\ M_{CZY} \end{bmatrix}$$

where $[T_S]$ is the steering law.

III. NORMAL MODE OF OPERATION

Cross-Product Steering Law

A careful examination of the expression for the reaction moment reveals that compensation for a disturbance torque can be accomplished by rotating the CMG momentum vector in the direction of the disturbance torque. Based on this, a steering law of the following form can be postulated:

$$\overline{\omega}_{VA(j)C} = K_{SL}\ \overline{1}_{2A(j)} X\ \overline{\alpha}_{TV}$$

where $\overline{\omega}_{VA(j)C}$ is the commanded j^{th} CMG momentum vector rate relative to vehicle space

K_{SL} is a constant

$\overline{1}_{2A(j)}$ is the unit vector along the spin vector of the j^{th} CMG

α_{TV} is a vector based on sensed information and indicates the direction of the disturbance torque.

Reference [2] derives the expression between the commanded gimbal rates and the commanded moment. This relationship is

$$\begin{bmatrix} \dot{\delta}_{1(1)C} \\ \dot{\delta}_{1(2)C} \\ \dot{\delta}_{1(3)C} \\ \dot{\delta}_{3(1)C} \\ \dot{\delta}_{3(2)C} \\ \dot{\delta}_{3(3)C} \end{bmatrix} = \begin{bmatrix} -C_{\delta 3(1)}S_{\delta 1(1)} & S_{\delta 3(1)}S_{\delta 1(1)} & -C_{\delta 1(1)} \\ -C_{\delta 1(2)} & -C_{\delta 3(2)}S_{\delta 1(2)} & S_{\delta 3(2)}S_{\delta 1(2)} \\ S_{\delta 3(3)}S_{\delta 1(3)} & -C_{\delta 1(3)} & -C_{\delta 3(3)}S_{\delta 1(3)} \\ -S_{\delta 3(1)} & -C_{\delta 3(1)} & 0 \\ 0 & -S_{\delta 3(2)} & -C_{\delta 3(2)} \\ -C_{\delta 3(3)} & 0 & -S_{\delta 3(3)} \end{bmatrix} \begin{bmatrix} M_{CXV} \\ M_{CYV} \\ M_{CZV} \end{bmatrix}$$

This steering law is referred to as the Cross-Product Steering Law.

If used directly for control of the CMG cluster, the Cross-Product Steering Law would be an open-loop scheme, and as such, would be unsatisfactory. A CMG cluster control law which provides closed-loop control of the cluster is developed in Reference [2]. This cluster control law is referred to as the H-Vector cluster control law. In this scheme, the moment command is integrated and compared with the angular momentum of the vehicle. The Cross-Product Steering Law then determines the six CMG gimbal angle rates required to drive the momentum error vector to zero. A single-axis block diagram of a CMG with the H-Vector control law is shown in Figure 4.

Figures 5, 6, 7, and 8 show, respectively, a momentum command for the x-axis, the CMG response for the x-axis, the momentum due to cross-coupling into the y-axis, and the momentum due to cross-coupling into the z-axis.

CMG Direct-Axis Bandwidth

The bandwidth of the CMG is an important quantity. In order to compensate adequately for disturbance torques, the bandwidth must be sufficiently large. Amplitude-frequency characteristics of a CMG are shown in Figure 9. The data for this curve was taken with the outer gimbal at 0° and the inner gimbal at +45°. The input was a sinusoidal signal to the inner gimbal rate loop. Because of the nonlinearities of the CMG, this does not represent a true frequency response. The data represents the ratio of the peak input signal to

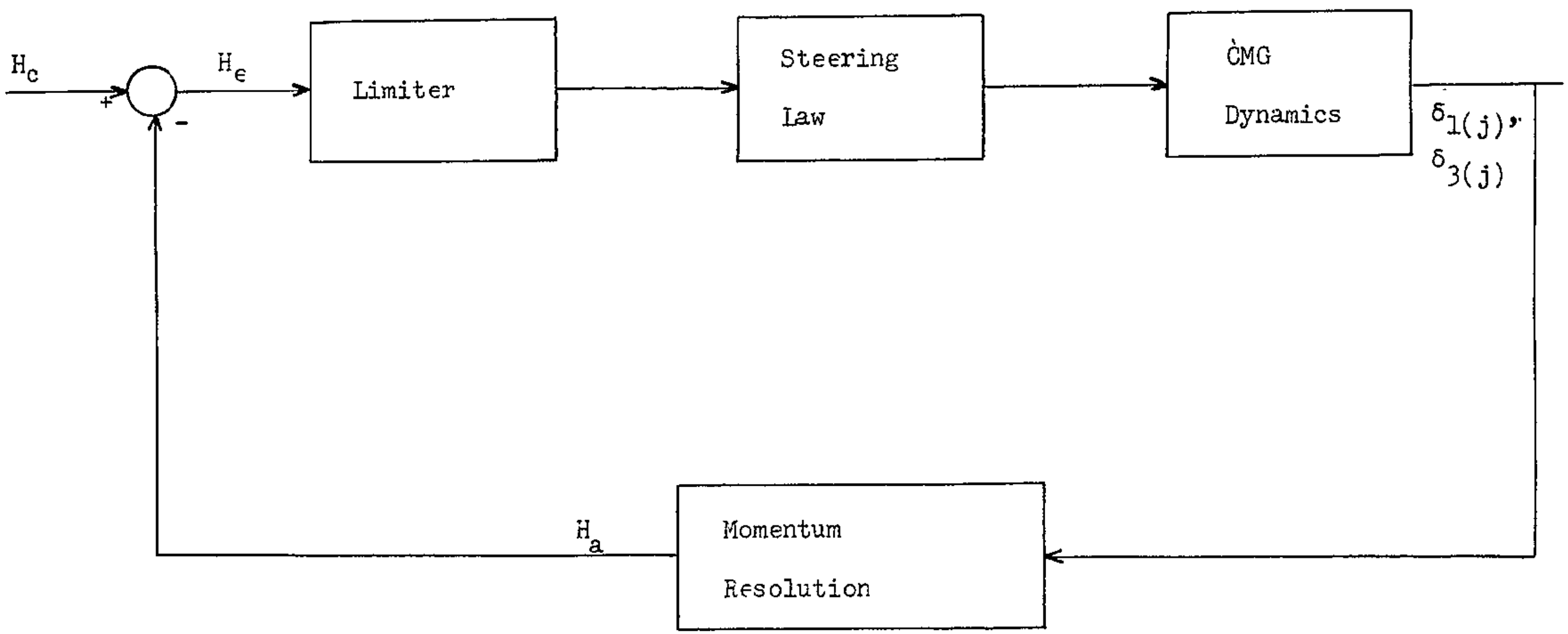

Figure 4. Single-Axis CMG Block Diagram

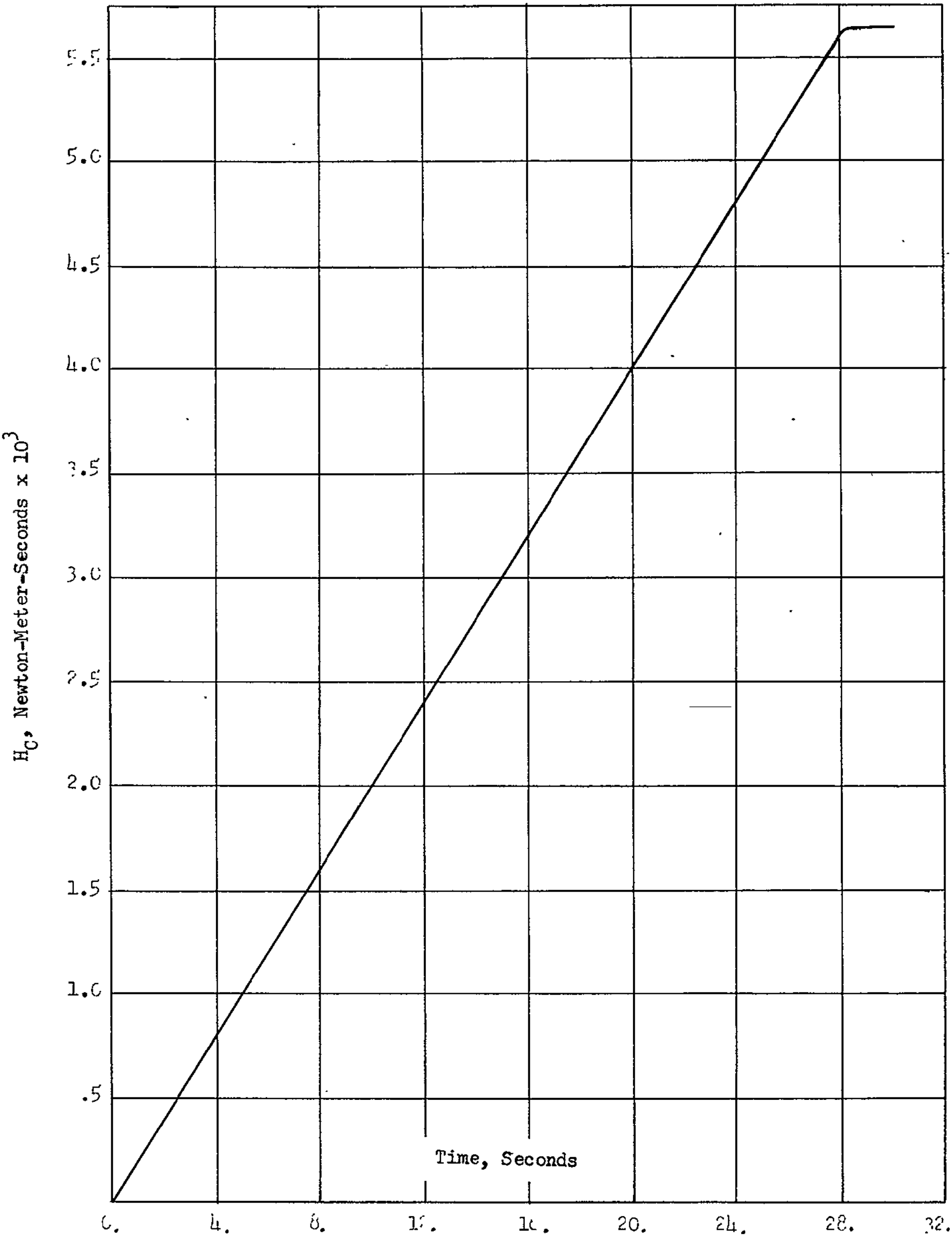

Figure 5. CMG Momentum Command, X-Axis

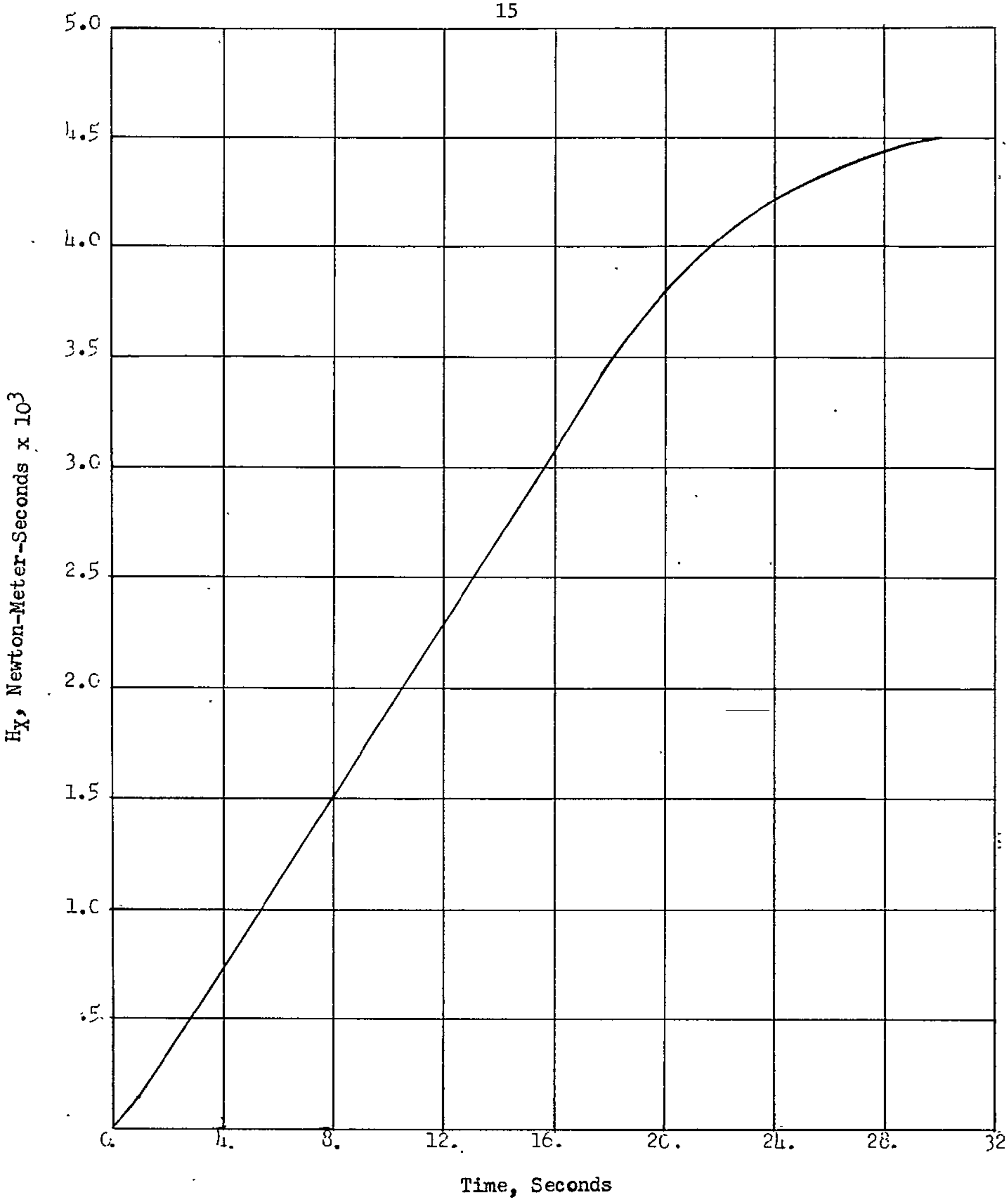

Figure 6. CMG Direct-Axis Response

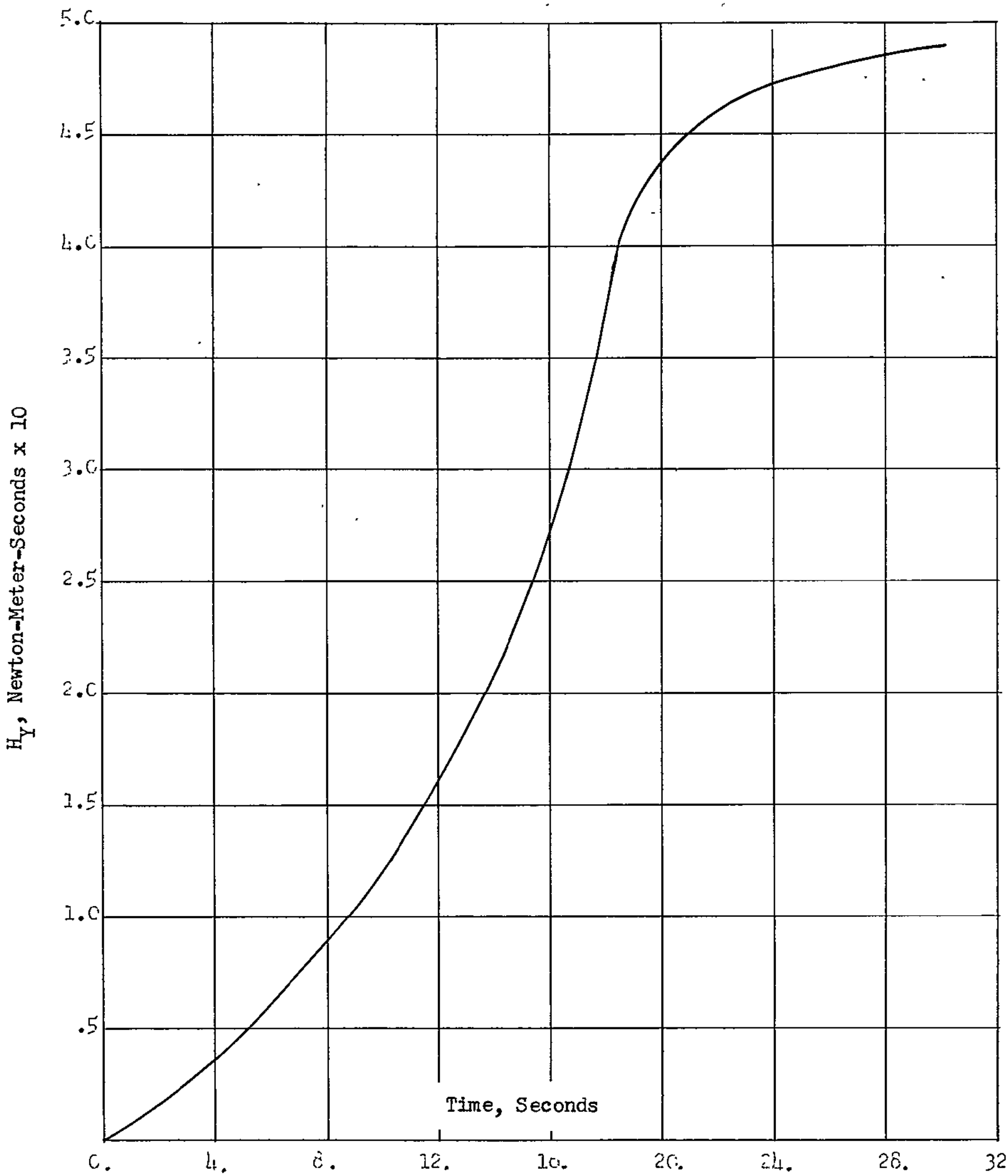

Figure 7. CMG Cross-Axis Response, Y-Axis

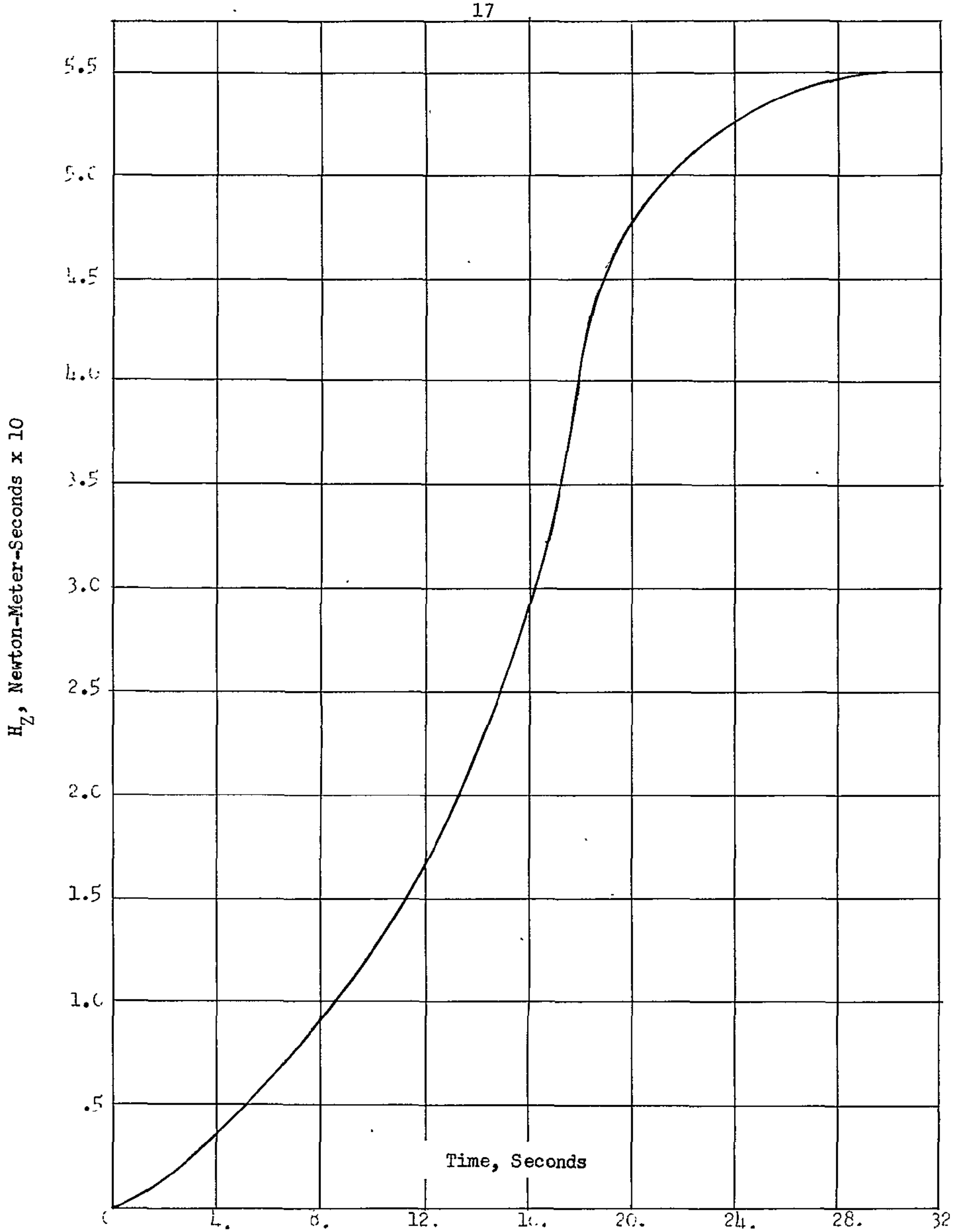

Figure 8. CMG Cross-Axis Response, Z-Axis

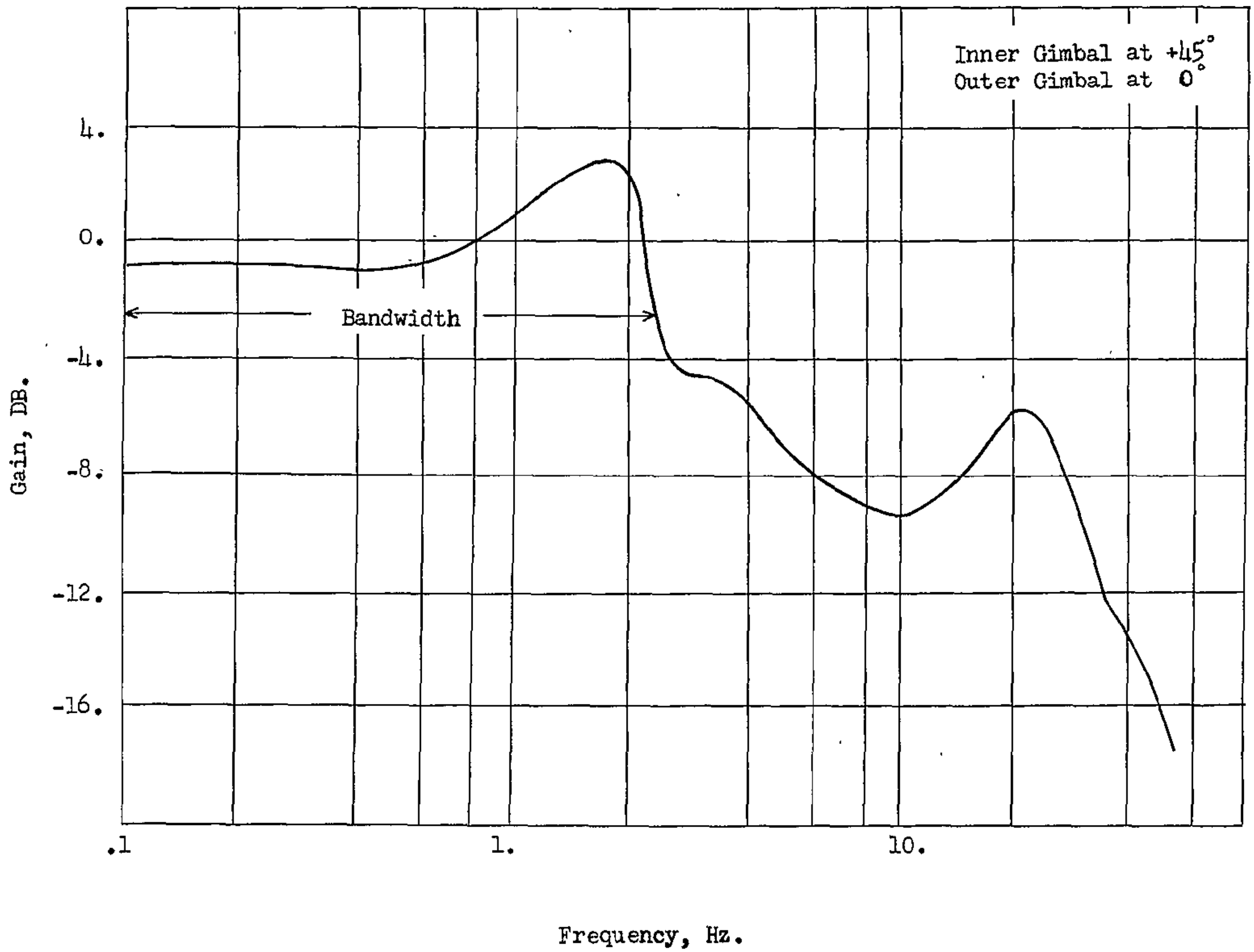

Figure 9. Unclamped CMG Amplitude-Frequency Characteristics

the peak output signal. As shown in Figure 9, the bandwidth is approximately 2.5 Hz.

Cross-Axis Response

An ideal steering law would determine the requirements necessary in order to exactly compensate for the disturbance torques. For example, for a disturbance torque in the x-axis only, in the ideal case, no reaction torque would be generated on the y and z axes. However, the Cross-Product Steering Law is not ideal and does generate reaction torques in other than the direct axis. Figures 10, 11, 12, and 13 show the reaction torques in the y and z axes and the x and z axes for a disturbance (initial condition in the x and y axes, respectively).

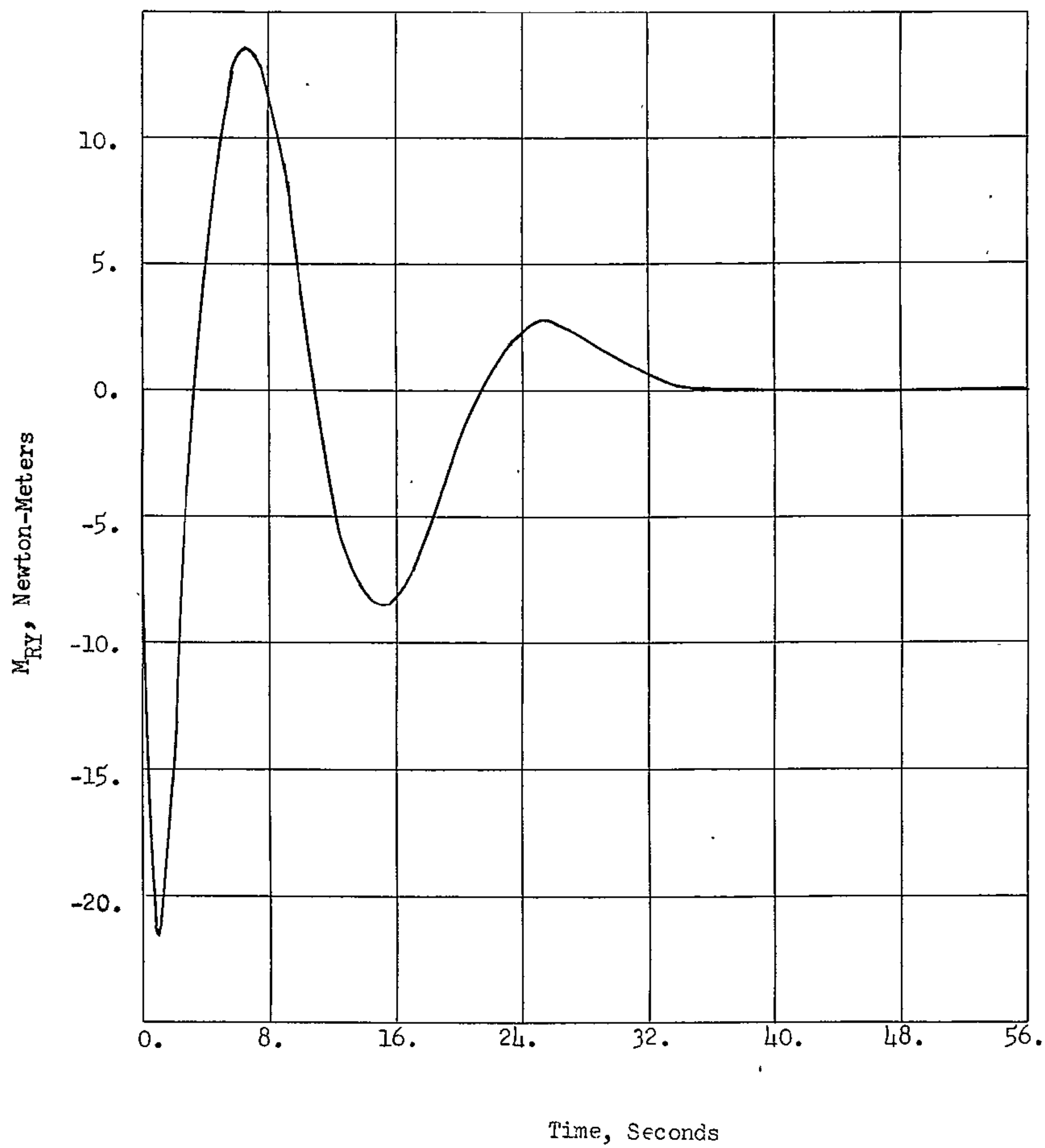

Figure 10. Reaction Moment, Y-Axis, Cross-Product Steering Law, Normal Mode, X-Axis Initial Condition

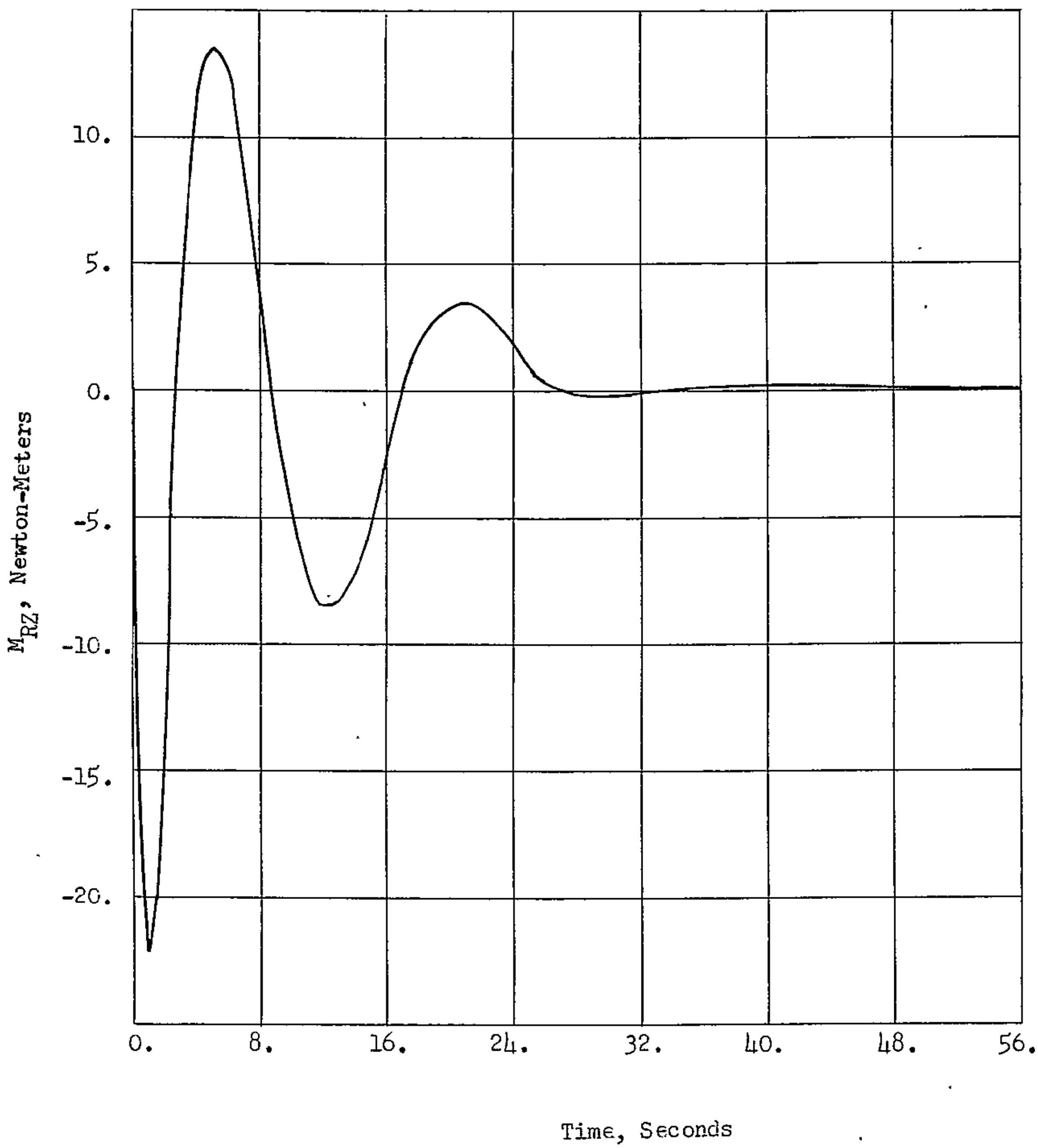

Figure 11. Reaction Moment, Z-Axis, Cross-Product Steering Law, Normal Mode, X-Axis Initial Condition

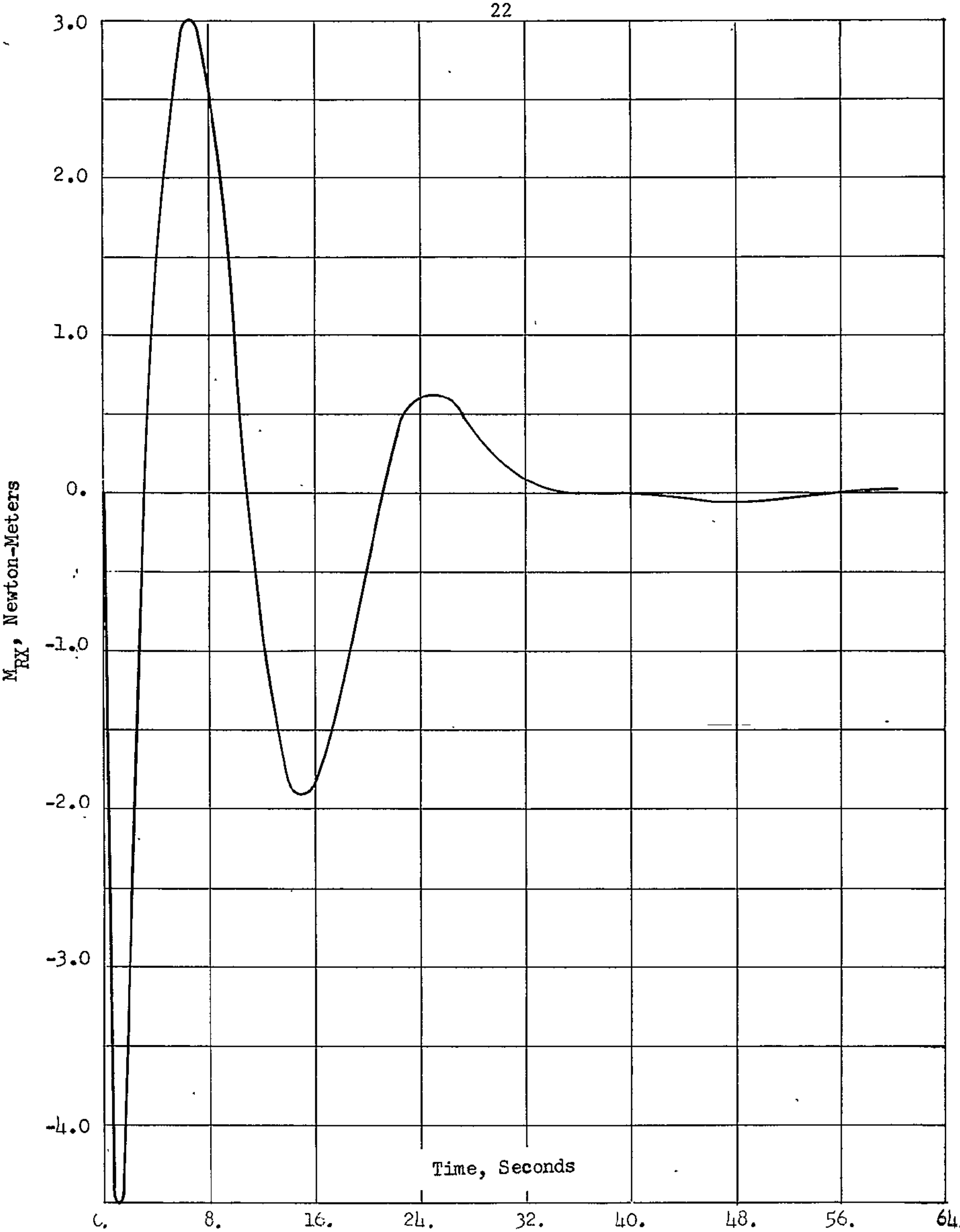

Figure 12. Reaction Moment, X-Axis, Cross-Product Steering Law, Normal Mode, Y-Axis Initial Condition

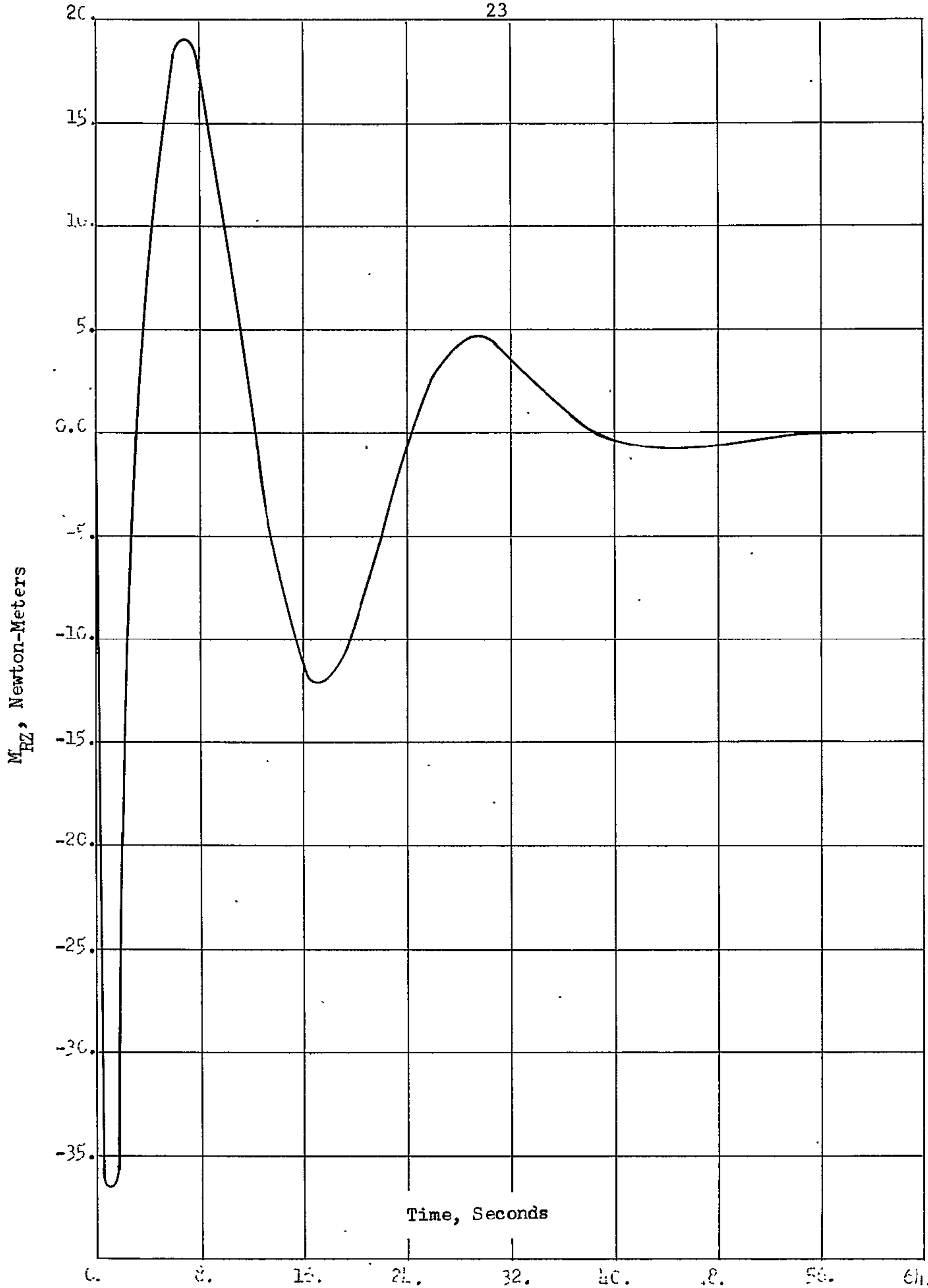

Figure 13. Reaction Moment, Z-Axis, Cross-Product Steering Law, Normal Mode, Y-Axis Initial Condition

IV. CLAMPED MODE OF OPERATION

This section presents a different technique for operation of the control system of the ATM. The technique consists essentially of rigidly clamping the outer gimbals to the frame and using the inner gimbals for dynamic control during certain periods of the flight, such as during the solar experiments. Prior to the the solar experiments, the outer gimbals are oriented so as to satisfy some specified criterion. This criterion will be discussed in a later section.

One of the significant advantages of the clamped mode of operation is that during the experimental periods when the outer gimbals are clamped, the inner to outer gimbal cross-coupling nonlinearities are eliminated. In addition, this method of operation results in a significant bandwidth increase for the control system.

From [3], the simplified equations for the dynamics of the inner and outer gimbals of a CMG are:

$$(sJ_{11} + N_g G_1)\dot{\delta}_1 - (H \operatorname{Cos}\delta_1 - G_{cc(1)})\dot{\delta}_3$$

$$= N_g G_1 \dot{\delta}_{1c} - sJ_1 \omega_{1c1c} - H \operatorname{Sin}\delta_1 \omega_{1c2c} + H \operatorname{Cos}\delta_1 \omega_{1B3B}$$

$$(H \operatorname{Cos}\delta_1 - G_{cc(3)})\dot{\delta}_1 + (sJ_{33} + N_g G_3)\dot{\delta}_3 = N_g G_3 \dot{\delta}_{3c}$$

$$- H \operatorname{Cos}\delta_1 \omega_{1c1c} - sJ_3 \omega_{1c2c} - sJ_2 \omega_{1B3B}$$

Assuming an input signal for $\dot{\delta}_{1c}$ only, the transfer function from $\dot{\delta}_{1c}$ to $\dot{\delta}_1$ is

$$\frac{\dot{\delta}_1}{\dot{\delta}_{1c}} = \frac{N_g G_1 (sJ_{33} + N_g G_3)}{\Delta}$$

where

$$\Delta = [(sJ_{11} + N_g G_1)(sJ_{33} + N_g G_3) + (HCos\delta_1 - Gcc(1)(HCos\delta_1 - Gcc(3)]$$

Optimal Steering Law

The equations for the reaction moment on the vehicle with the gyros in the clamped mode of operation may be found from the equations derived previously. With the outer gimbals clamped, the outer gimbal rates $\dot{\delta}_{3(1)}$, $\dot{\delta}_{3(2)}$, and $\dot{\delta}_{3(3)}$ are zero. The equations for the reaction moments, in matrix form, are:

$$\begin{bmatrix} M_{RXV} \\ M_{RYV} \\ M_{RZV} \end{bmatrix} = \begin{bmatrix} S\delta_{1(1)}\, C\delta_{3(1)} & C\delta_{1(2)} & -S\delta_{1(3)}\, S\delta_{3(3)} \\ -S\delta_{1(1)}\, S\delta_{3(1)} & S\delta_{1(2)}\, C\delta_{3(2)} & C\delta_{1(3)} \\ C\delta_{1(1)} & -S\delta_{1(2)}\, S\delta_{3(2)} & S\delta_{1(3)}\, C\delta_{3(3)} \end{bmatrix} \begin{bmatrix} \dot{\delta}_{1(1)} \\ \dot{\delta}_{1(2)} \\ \dot{\delta}_{1(3)} \end{bmatrix}$$

The relationship between the commanded moment and the commanded gimbal rates is

$$\begin{bmatrix} \dot{\delta}_{1(1)C} \\ \dot{\delta}_{1(2)C} \\ \dot{\delta}_{1(3)C} \end{bmatrix} = [T_s] \begin{bmatrix} M_{CXV} \\ M_{CYV} \\ M_{CZV} \end{bmatrix}$$

Assuming that the actual gimbal rates are equal to the commanded gimbal rates, the relationship between the commanded moment and the reaction moment is:

$$\begin{bmatrix} M_{RXV} \\ M_{RYV} \\ M_{RZV} \end{bmatrix} = [A]\ [T_s] \begin{bmatrix} M_{CXV} \\ M_{CYV} \\ M_{CZV} \end{bmatrix}$$

where [A] is the matrix relating the reaction moments on the vehicle to the CMG gimbal rates. In order to optimally control the CMG cluster, it is necessary that the reaction moment be equal to the commanded moment. In equation form, this condition may be stated as:

$$[A]\ [T_s] = [I]$$

The steering law $[T_s]$ that satisfies this condition is given by:

$$[T_s] = [A]^{-1},$$

where $[\ \ ]^{-1}$ denotes the inverse. Assuming $[T_s]$ is of the form

$$[T_s] = \begin{bmatrix} T_{11} & T_{12} & T_{13} \\ T_{21} & T_{22} & T_{23} \\ T_{31} & T_{32} & T_{33} \end{bmatrix},$$

the solution for the optimal steering law is:

$$T_{11} = \frac{1}{\Delta}\,[S\delta_{1(2)}\ C\delta_{3(2)}\ C\delta_{3(3)}\ S\delta_{1(3)} + S\delta_{1(2)}\ S\delta_{3(2)}\ C\delta_{1(3)}]$$
$$T_{12} = \frac{1}{\Delta}\,[-C\delta_{1(2)}\ C\delta_{3(3)}\ S\delta_{1(3)} + S\delta_{1(2)}\ S\delta_{3(2)} S\delta_{3(3)}\ S\delta_{1(3)}]$$
$$T_{13} = \frac{1}{\Delta}\,[C\delta_{1(2)}\ C\delta_{1(3)} + S\delta_{1(2)}\ C\delta_{3(2)}\ S\delta_{3(3)}\ S\delta_{1(3)}]$$
$$T_{21} = \frac{1}{\Delta}\,[S\delta_{3(1)}\ S\delta_{1(1)}\ C\delta_{3(3)}\ S\delta_{1(3)} + C\delta_{1(1)}\ C\delta_{1(3)}]$$
$$T_{22} = \frac{1}{\Delta}\,[C\delta_{3(1)}\ S\delta_{1(1)}\ C\delta_{3(3)}\ S\delta_{1(3)} + C\delta_{1(1)}\ S\delta_{3(3)}\ S\delta_{1(3)}]$$
$$T_{23} = \frac{1}{\Delta}\,[-C\delta_{3(1)}\ S\delta_{1(1)}\ C\delta_{1(3)} + S\delta_{1(3)}\ S\delta_{1(1)}\ S\delta_{3(3)}\ S\delta_{1(3)}]$$
$$T_{31} = \frac{1}{\Delta}\,[S\delta_{3(1)}\ S\delta_{1(1)}\ S\delta_{1(2)}\ S\delta_{3(2)} - C\delta_{1(1)}\ S\delta_{1(2)}\ C\delta_{3(2)}]$$
$$T_{32} = \frac{1}{\Delta}\,[C\delta_{3(1)}\ S\delta_{1(1)}\ S\delta_{1(2)}\ S\delta_{3(2)} - C\delta_{1(1)}\ C\delta_{1(2)}]$$
$$T_{33} = \frac{1}{\Delta}\,[C\delta_{3(1)}\ S\delta_{1(1)}\ S\delta_{1(2)}\ C\delta_{3(2)} + S\delta_{3(1)}\ S\delta_{1(1)}\ C\delta_{1(2)}]$$

where

$$\begin{aligned}\Delta = H[&(C\delta_{3(1)}\ S\delta_{1(1)}\ S\delta_{1(2)}\ C\delta_{3(2)}\ C\delta_{3(3)}\ S\delta_{1(3)})\\ &-(S\delta_{3(1)}\ S\delta_{1(1)}\ S\delta_{1(2)}\ S\delta_{3(2)}\ S\delta_{3(3)}\ S\delta_{1(3)})\\ &+(C\delta_{1(1)}\ C\delta_{1(3)}\ C\delta_{1(2)}) + (C\delta_{1(1)}\ S\delta_{1(2)}\ C\delta_{3(2)}\ S\delta_{3(3)}\ S\delta_{1(3)})\\ &+(S\delta_{1(2)}\ S\delta_{3(2)}\ C\delta_{1(3)}\ C\delta_{3(1)}\ S\delta_{1(1)})\\ &+(C\delta_{3(3)}\ S\delta_{1(3)}\ C\delta_{1(2)}\ S\delta_{3(1)}\ S\delta_{1(1)}].\end{aligned}$$

CMG Direct-Axis Bandwidth

As shown previously, the direct-axis bandwidth of a CMG in normal operation is approximately 2.5 Hz. Figure 14 shows the amplitude vs. frequency characteristics of a CMG in normal operation and also for a CMG in the clamped mode of operation [3]. The data for both curves was taken with the inner gimbal at +45° and with the outer gimbal at 0°. However, for the clamped mode of operation, the outer gimbal was clamped to the frame. As in the previous case, the input was a sinusoidal signal to the inner gimbal rate loop, and the data represents the ratio of the peak output signal to the peak input signal. As can be seen in the Figure, the bandwidth of the CMG is significantly increased by clamping the outer gimbal to the frame. The bandwidth of the CMG in the clamped mode of operation is approximately 5.9 Hz.

Cross-Axis Response

As stated previously, an ideal steering law would determine the necessary requirements in order to compensate exactly for the disturbance torques. The Optimal Steering Law closely approaches the

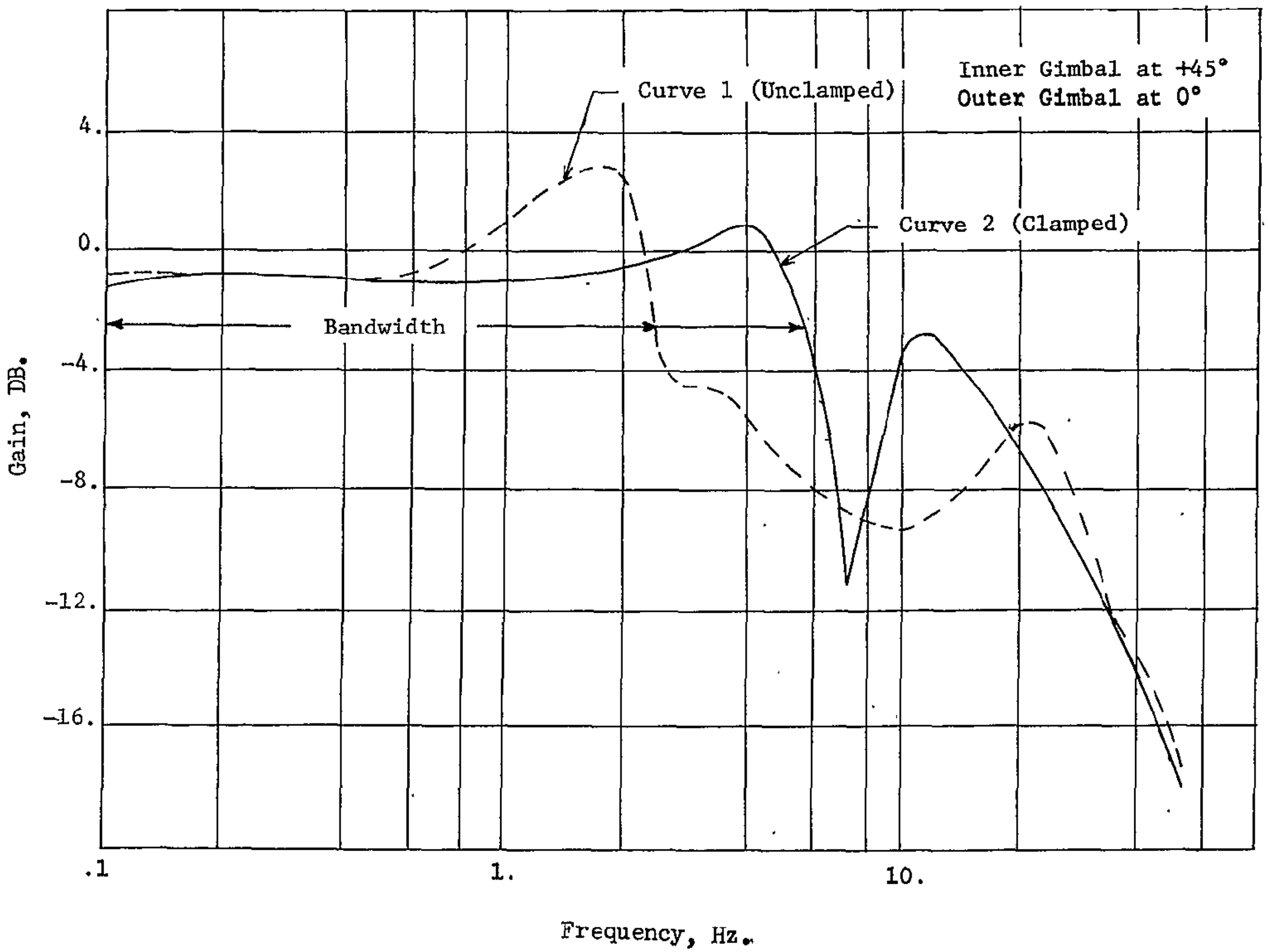

Figure 14. Clamped and Unclamped CMG Amplitude-Frequency Characteristics

ideal situation as only small reaction moments are generated in other than the direct axis. Figures 15, 16, 17 and 18 show the reaction torques in the y and z axes and the x and z axes for a disturbance (initial condition in the x and y axes, respectively).

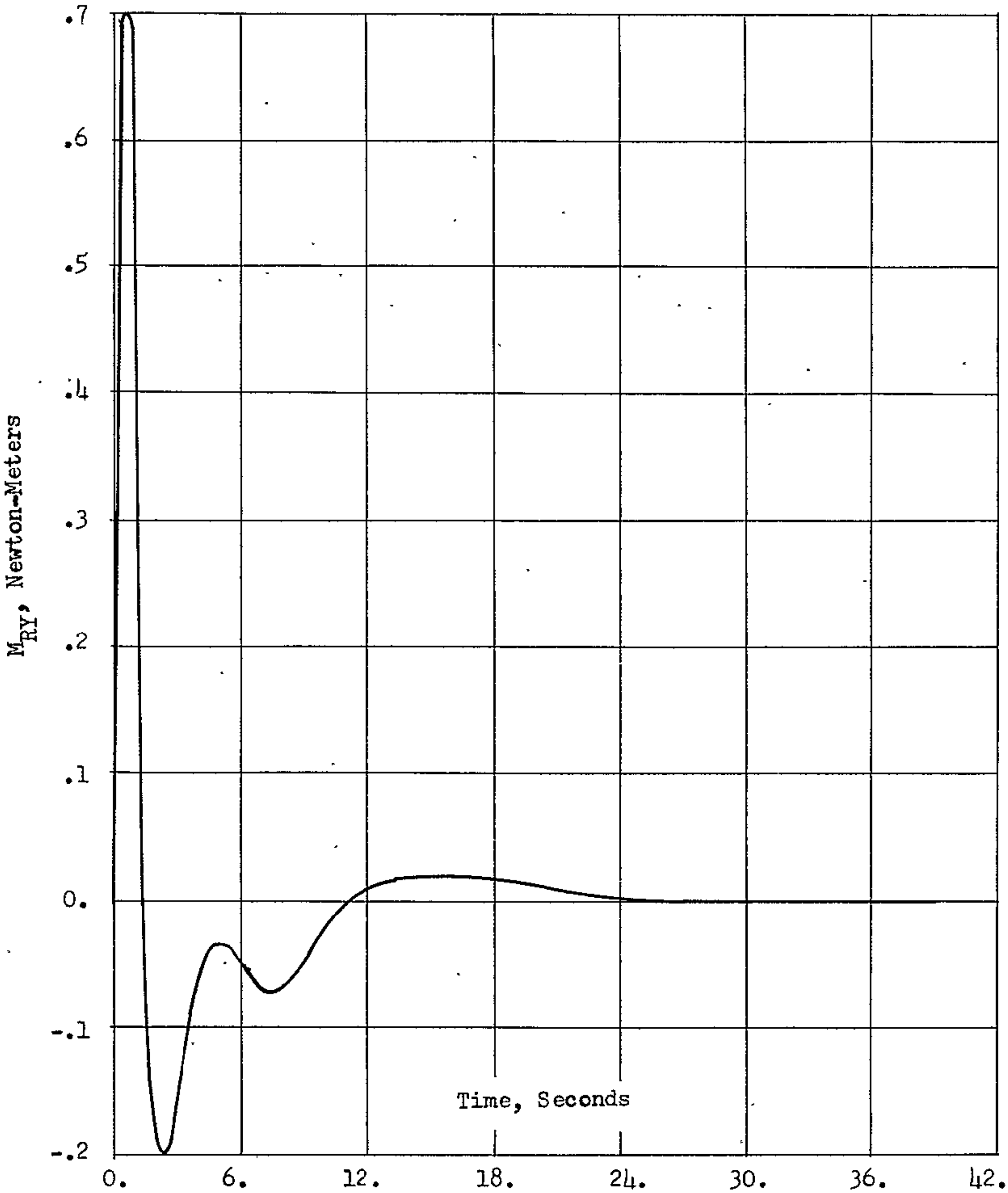

Figure 15. Reaction Moment, Y-Axis, Optimal Steering Law, Clamped Mode, X-Axis Initial Condition

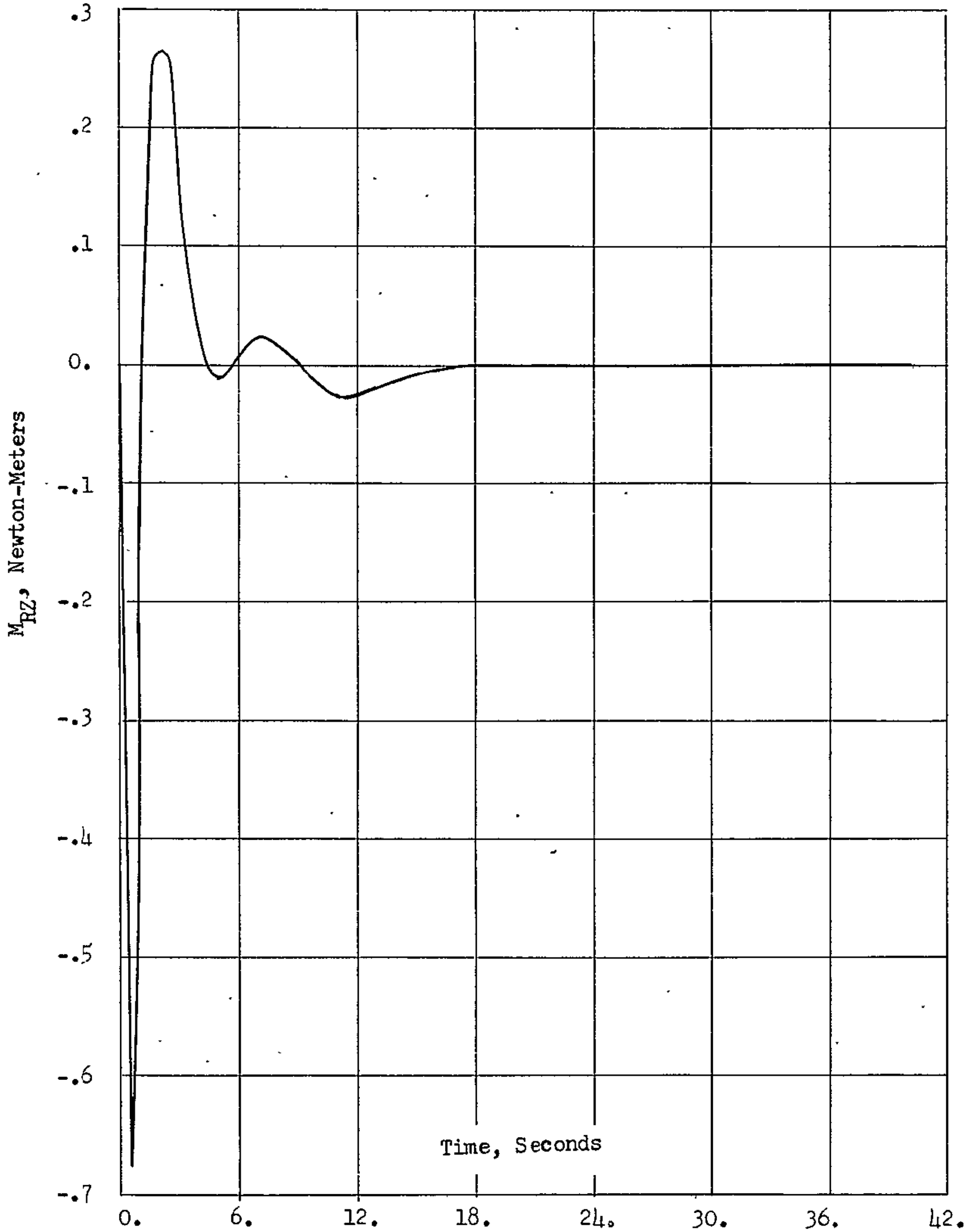

Figure 16. Reaction Moment, Z-Axis, Optimal Steering Law, Clamped Mode, X-Axis Initial Condition

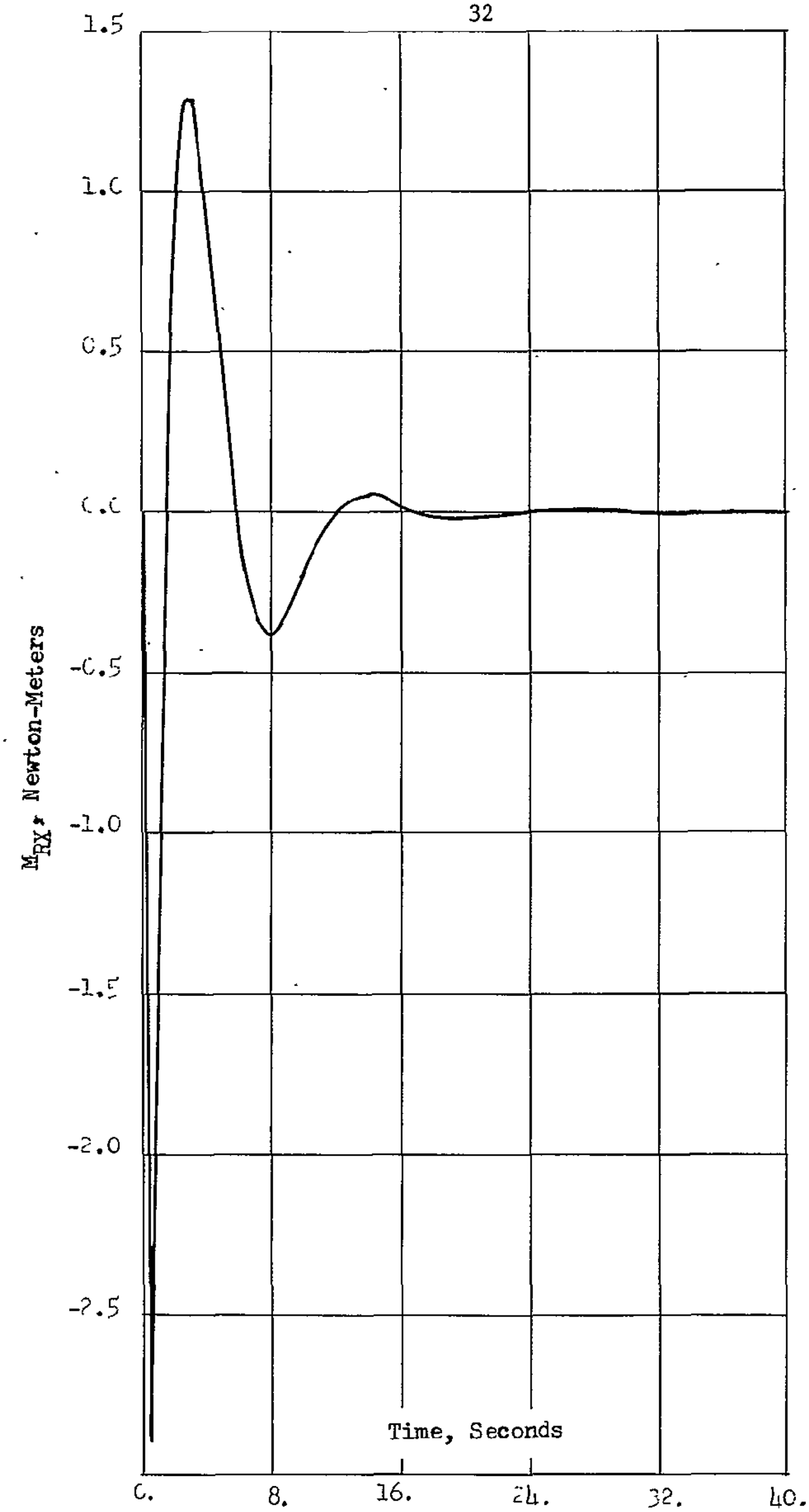

Figure 17. Reaction Moment, X-Axis, Optimal Steering Law, Clamped Mode, Y-Axis Initial Condition

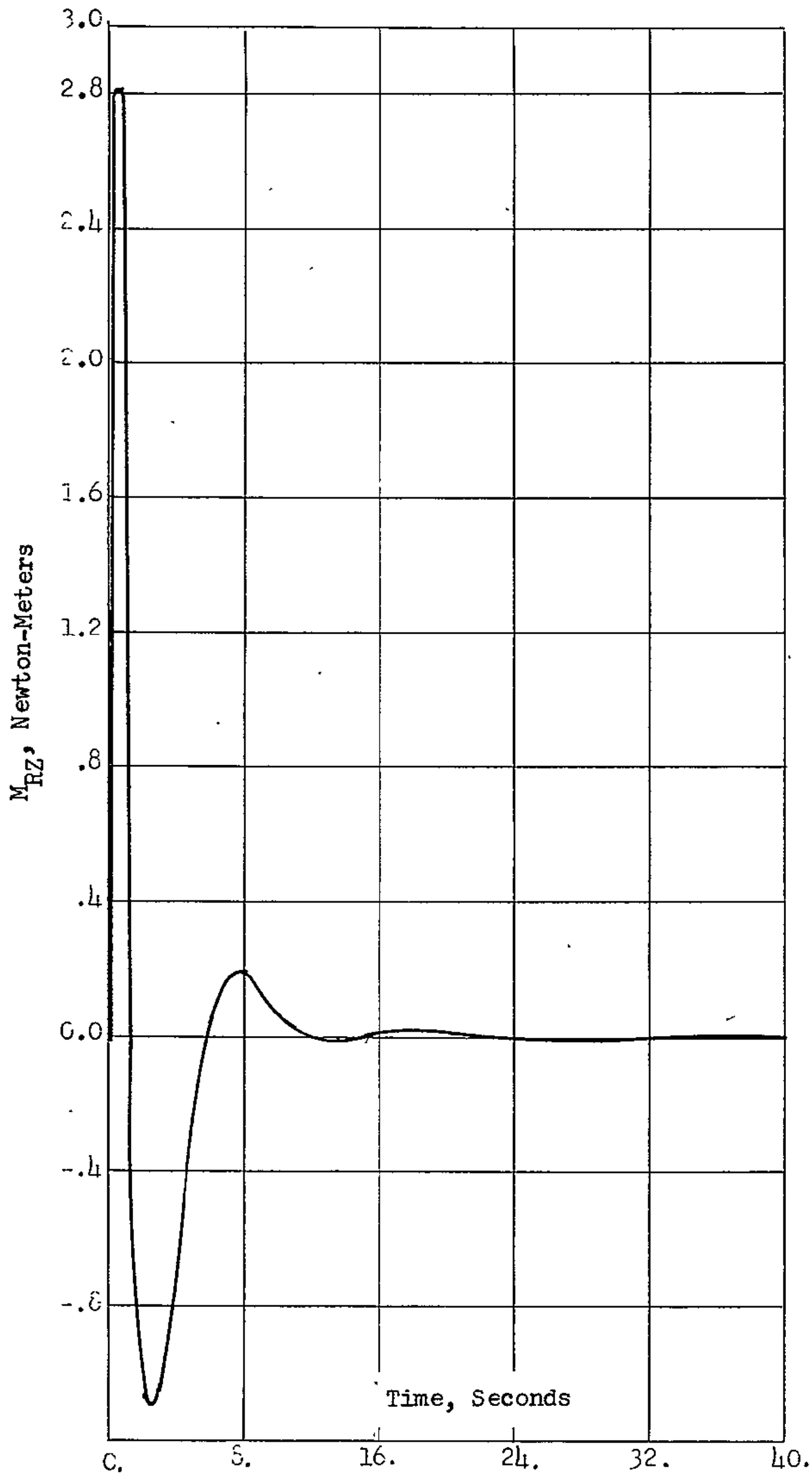

Figure 18. Reaction Moment, Z-Axis, Optimal Steering Law, Clamped Mode, Y-Axis Initial Condition

V. STUDY RESULTS

Dynamic Response Characteristics

Results obtained from simulation studies of the ATM system in order to determine the dynamic response characteristics of the various system configurations are presented in this section.

Normal Mode, Cross-Product Steering Law

There is one vehicle control loop for each of the three control axes. A single-axis block diagram for one of the vehicle control loops is shown in Figure 19. The vehicle control loop has a rate-plus-position control law. As illustrated in Figure 19, the vehicle control law output is processed and integrated in order to obtain the momentum command for the inner loop. This command signal is compared to the vehicle momentum and the error is used to generate the gimbal rates required to provide the proper reaction moment on the vehicle.

Figures 20, 21, and 22 show the response of the x-axis of the system, the y-axis of the system, and the z-axis of the system due to an initial condition in the x-axis, the y-axis, and the z-axis, respectively.

Clamped Mode, Cross-Product Steering Law

This section presents the results obtained from simulation studies of the system with the CMG's in the clamped mode. For each of the

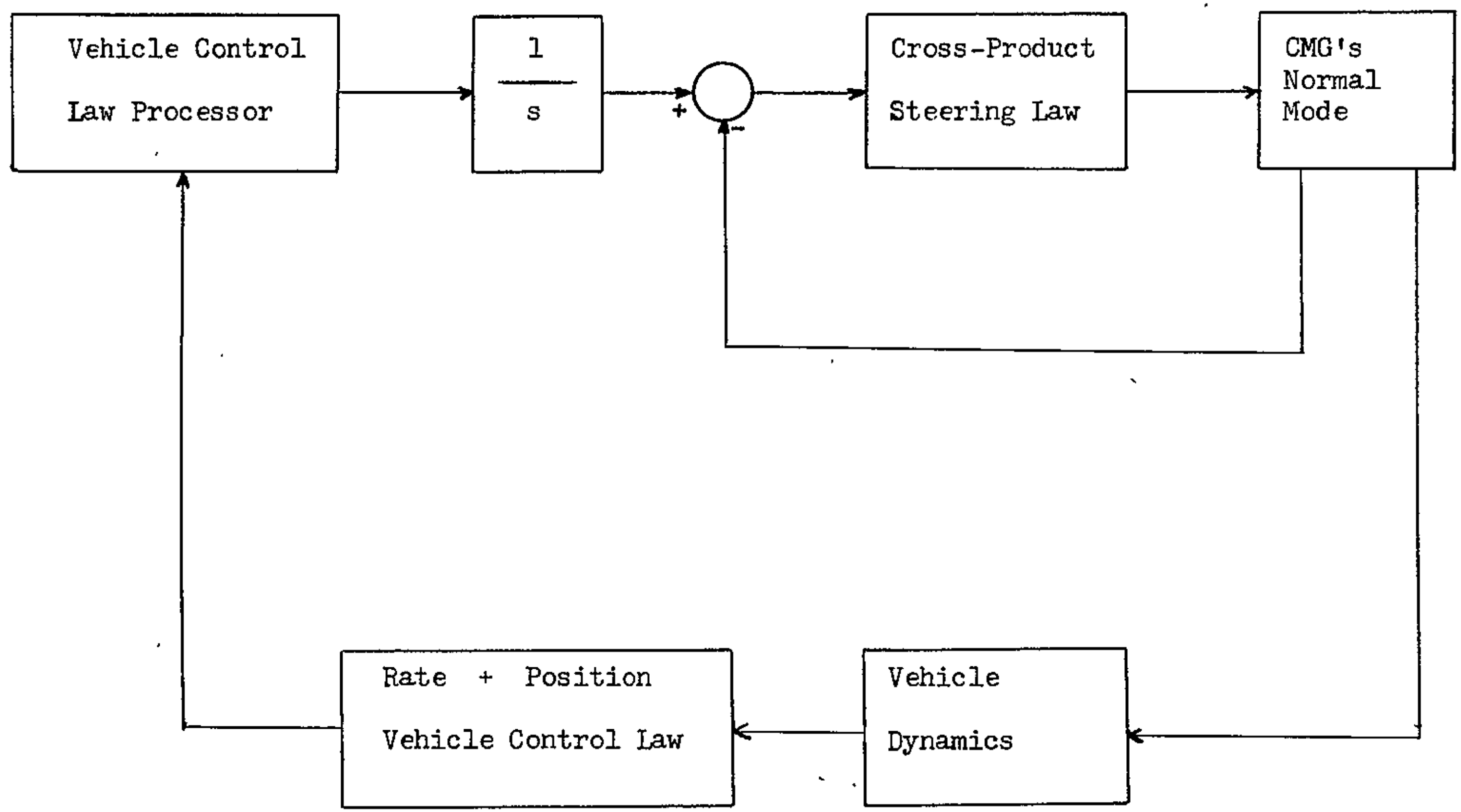

Figure 19. Single-Axis Block Diagram, Cross-Product Steering Law, Normal Mode

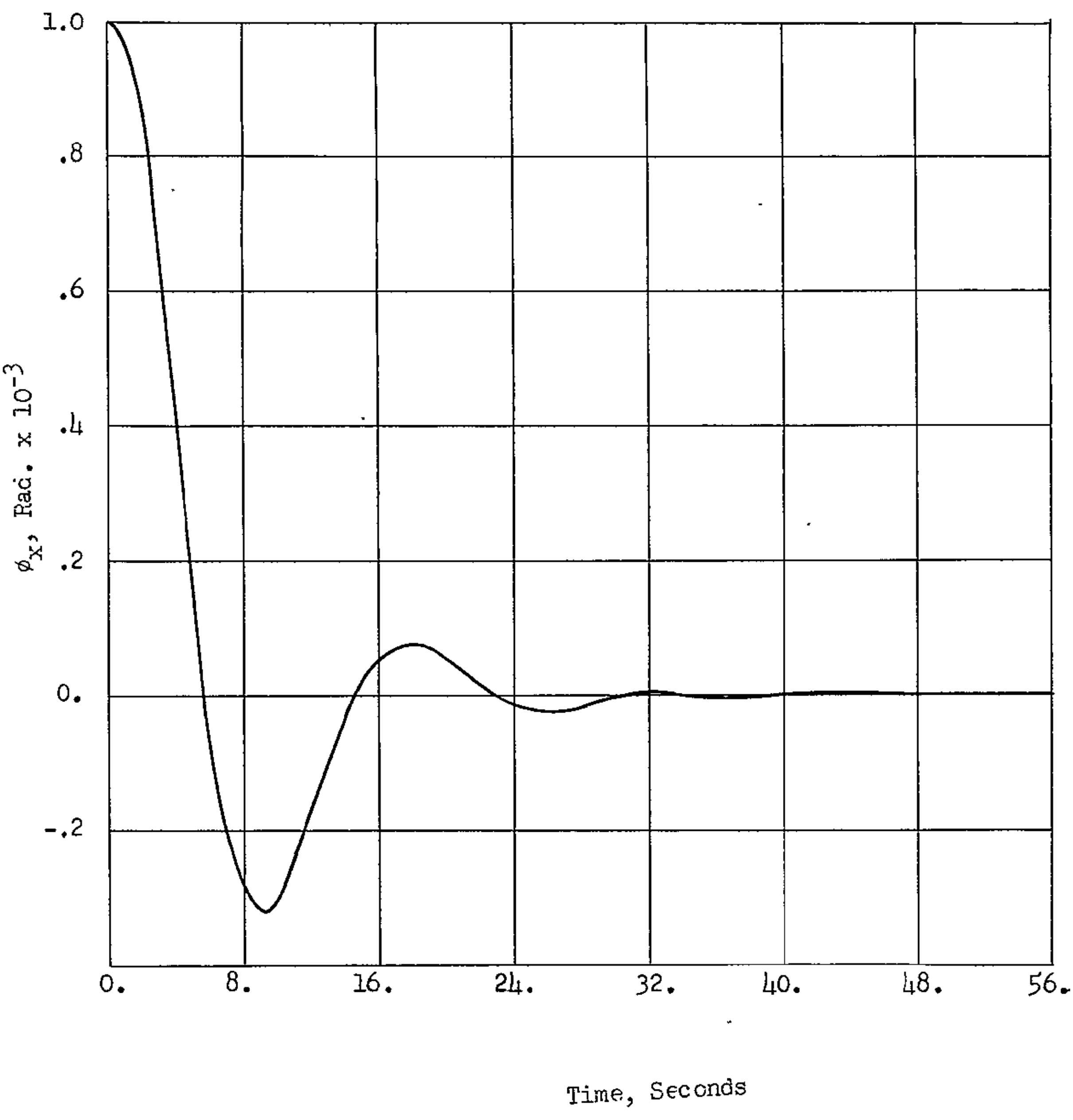

Figure 20. X-Axis Response, Cross-Product Steering Law, Normal Mode

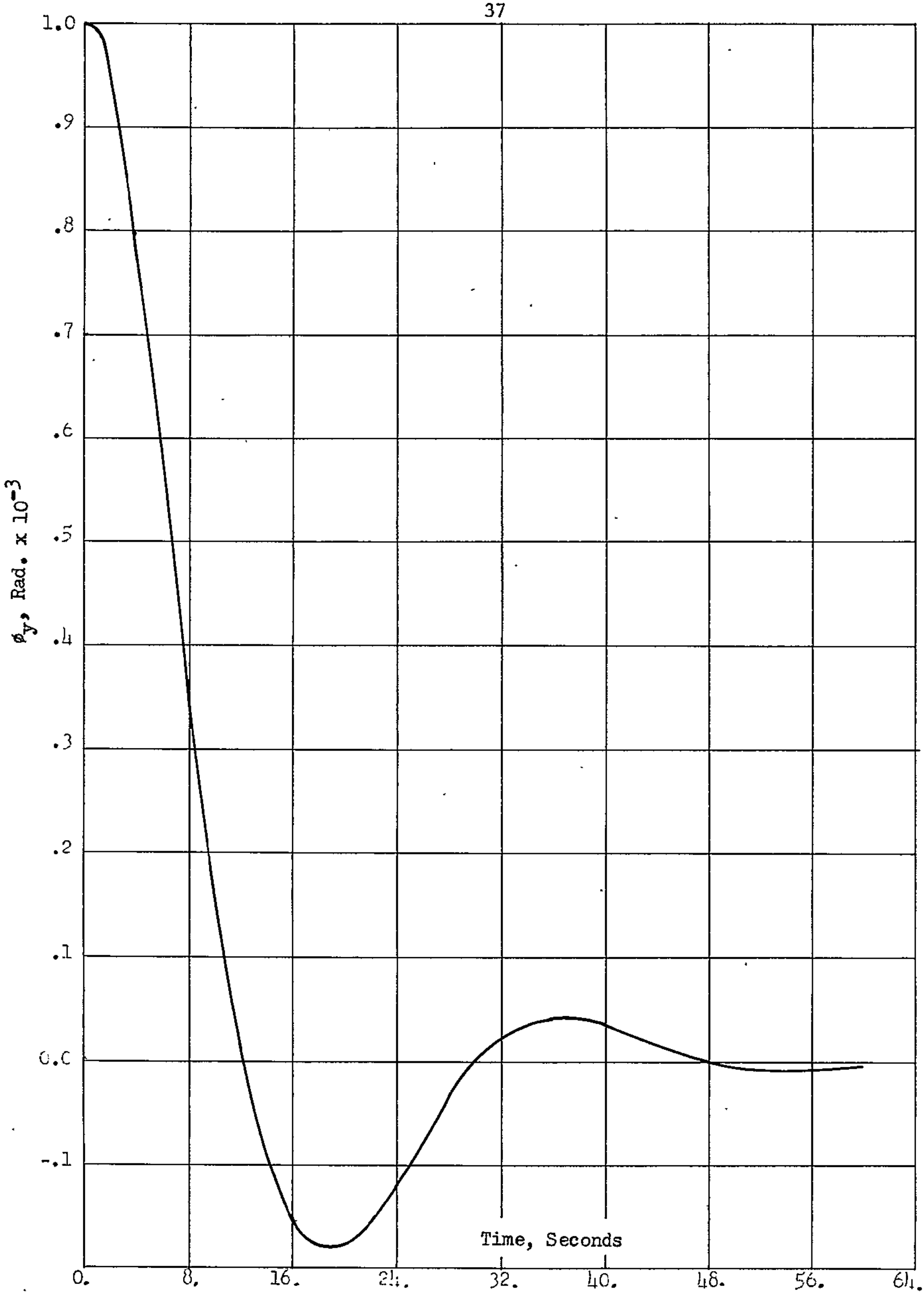

Figure 21. Y-Axis Response, Cross-Product Steering Law, Normal Mode

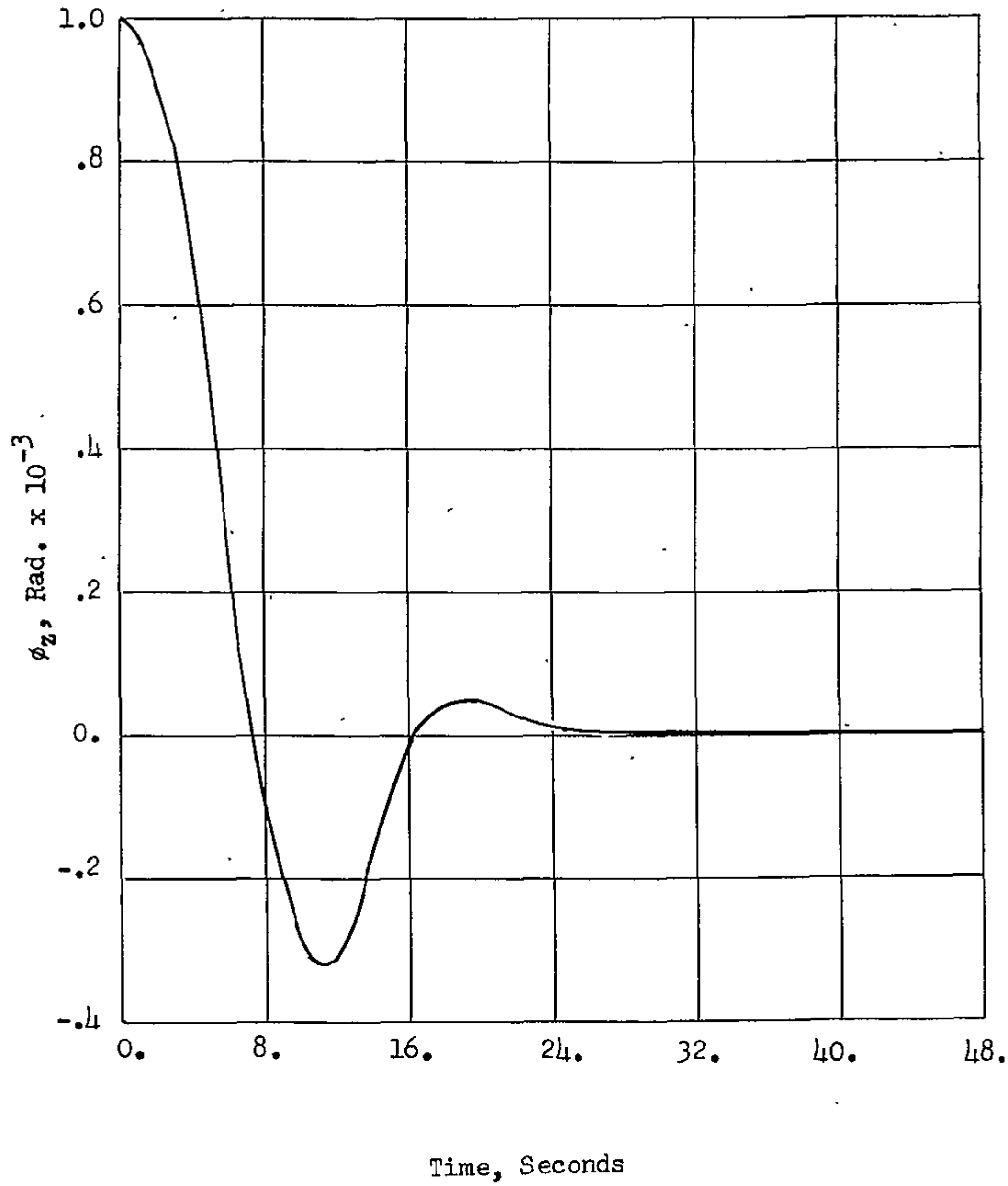

Figure 22. Z-Axis Response, Cross-Product Steering Law, Normal Mode

control axes, there is one vehicle control loop. A single-axis block diagram for one of the vehicle control loops with the CMG's in the clamped mode and using the Cross-Product Steering Law is shown in Figure 23. A rate-plus-position control law is used for each of the vehicle control loops. As in the previous case with the CMG's in the normal mode of operation, the vehicle control law output is processed and integrated to obtain the momentum command for the inner loop. This momentum command is compared to the actual vehicle momentum and the difference is used to provide the proper reaction moment on the vehicle.

Figures 24, 25, and 26 show the response of the x-axis, the y-axis, and the z-axis of the system due to an initial condition in the x-axis, the y-axis, and the z-axis, respectively.

Clamped Mode, Optimal Steering Law

Results are presented here which were obtained from simulation studies of the ATM system using the Optimal Steering Law with the CMG's in the clamped mode of operation. As in the previous system configurations, there is one vehicle control loop for each of the control axes. The cluster control law used for this system configuration is a Moment Control Law. A block diagram for one of the vehicle control loops with the CMG's in the clamped mode of operation and with the Optimal Steering Law is shown in Figure 27. A rate-plus-position control law is used for each of the vehicle control loops. For this system configuration, the vehicle control law output is processed in order to obtain the moment command for the inner loop. This moment command is compared to the actual moment and the error is used,

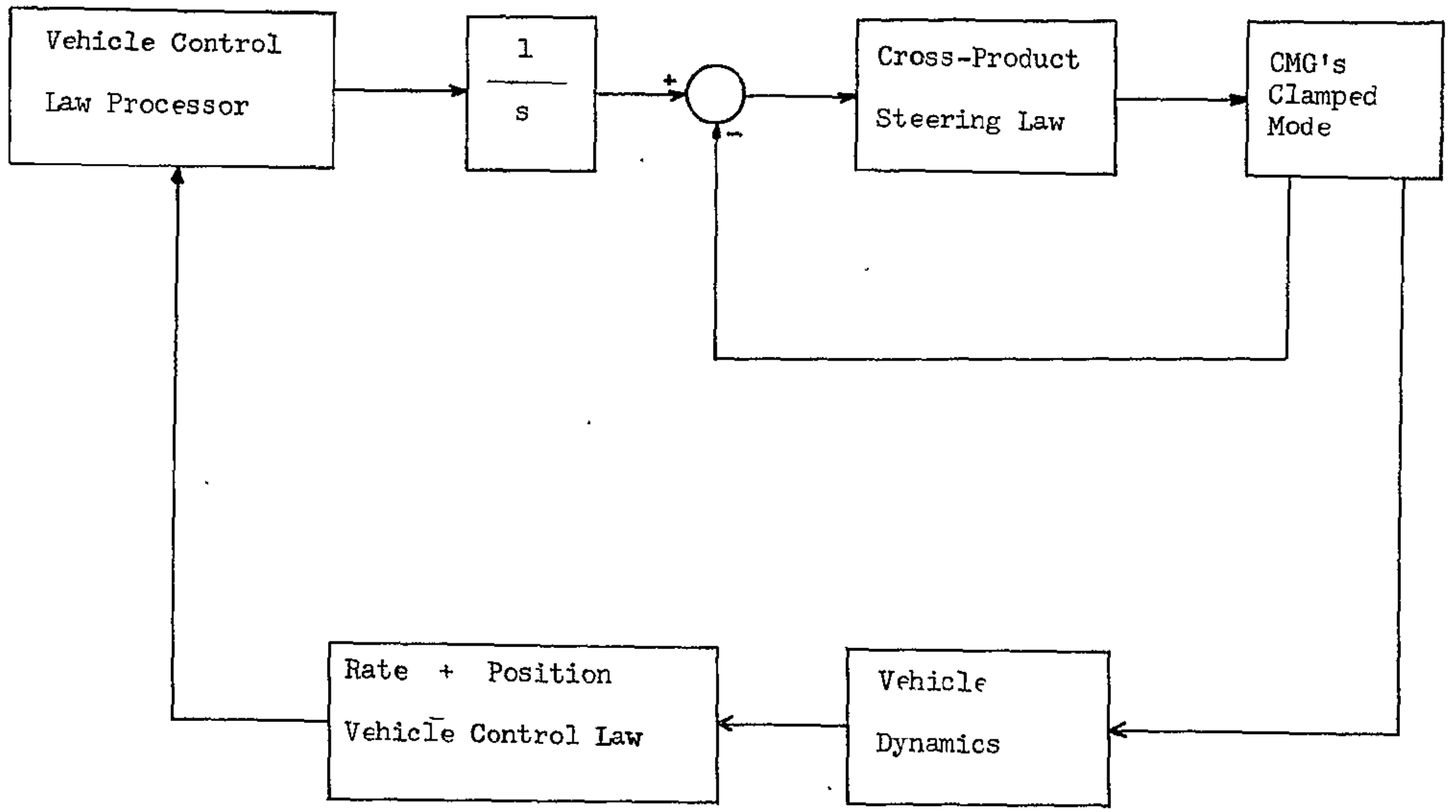

Figure 23. Single-Axis Block Diagram, Cross-Product Steering Law, Clamped Mode

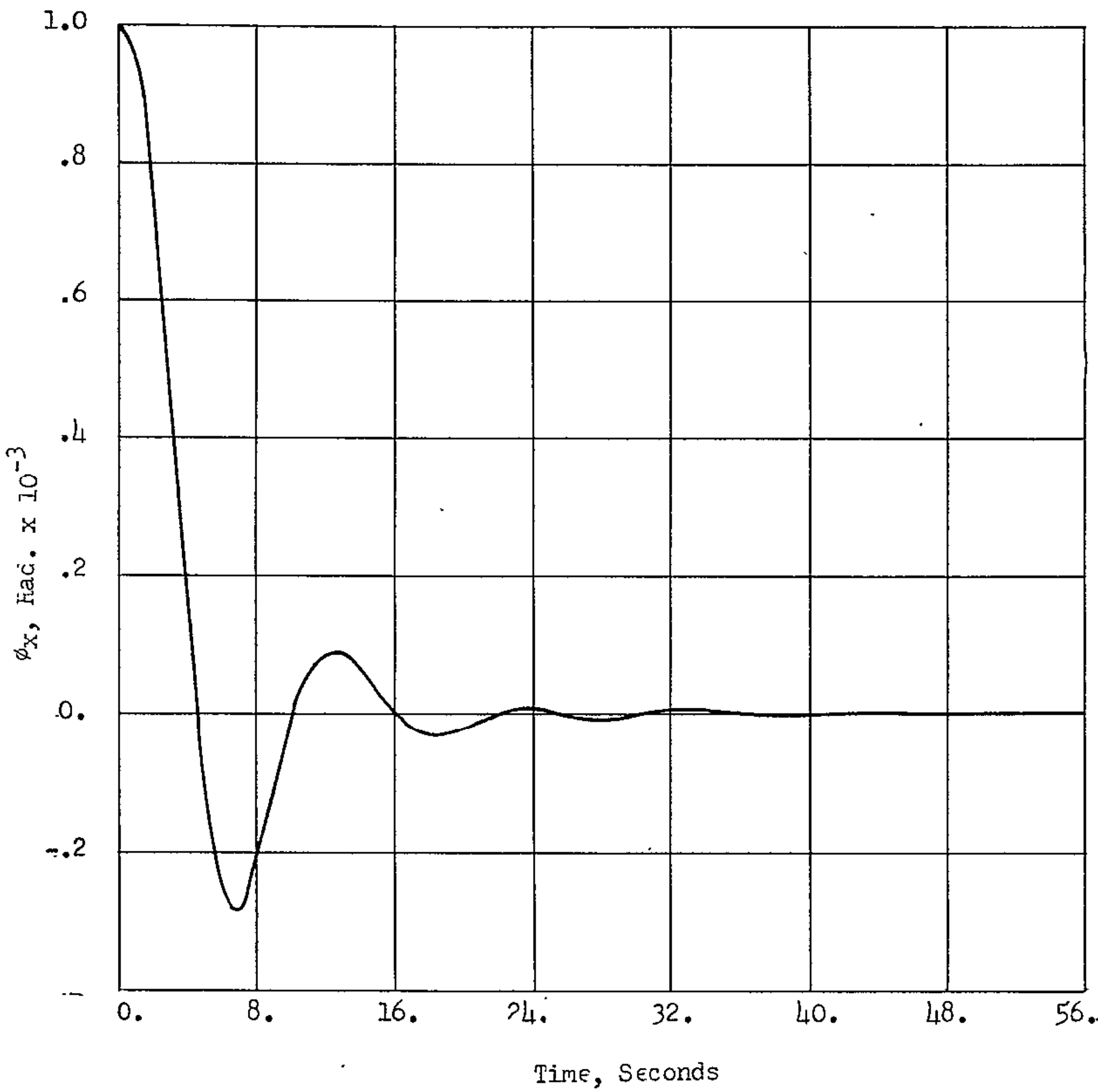

Figure 24. X-Axis Response, Cross-Product Steering Law, Clamped Mode

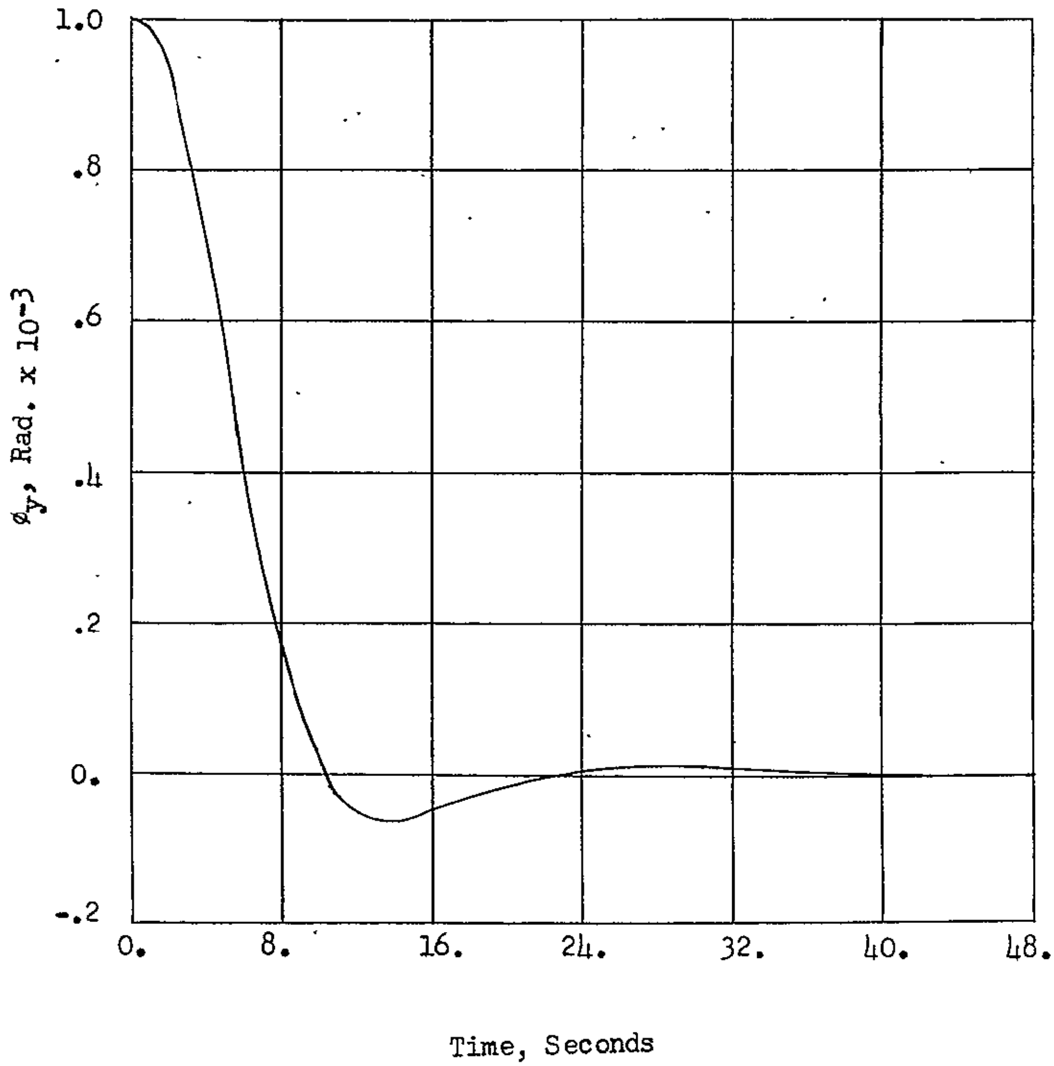

Figure 25. Y-Axis Response, Cross-Product Steering Law, Clamped Mode

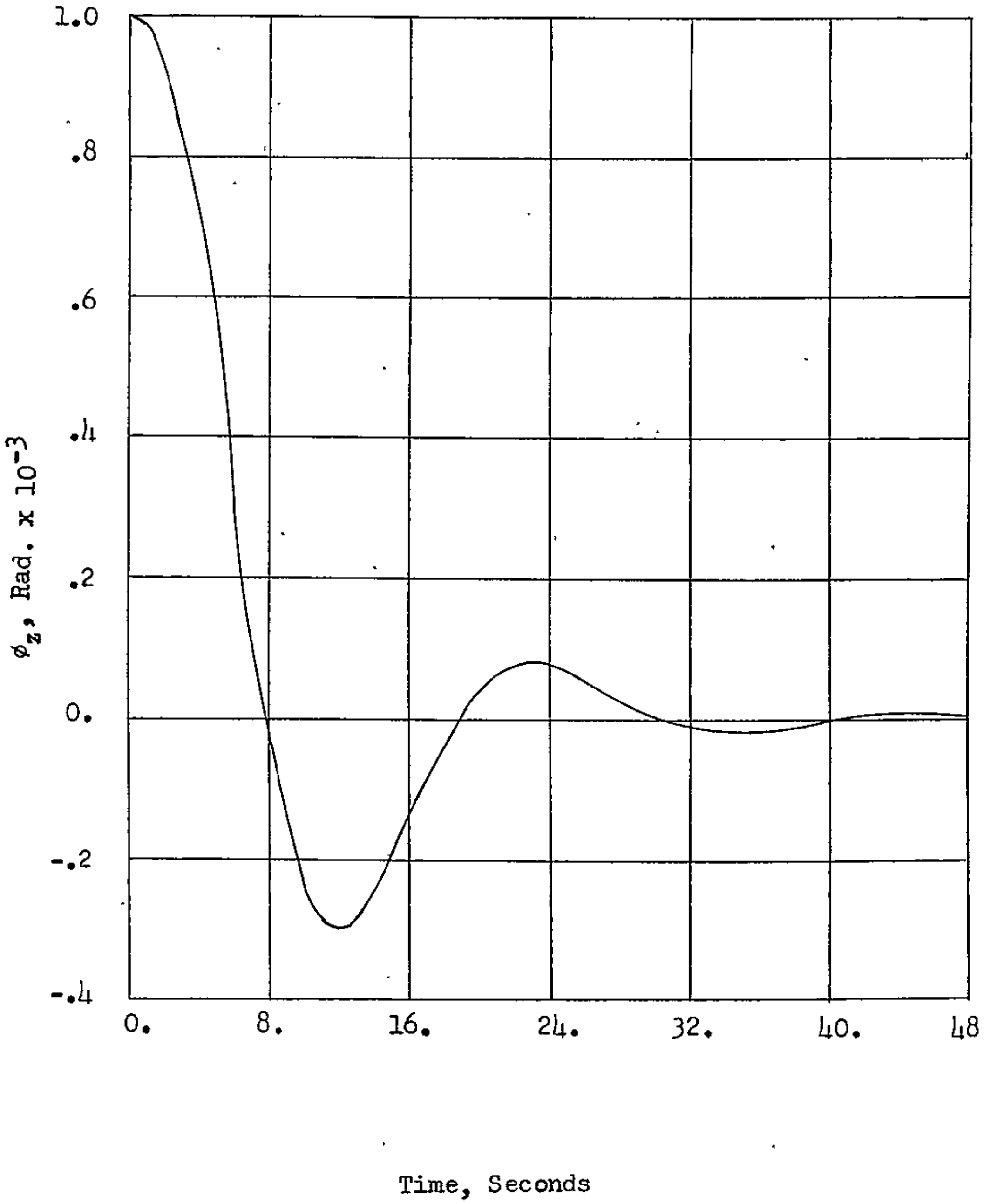

Figure 26. Z-Axis Response, Cross-Product Steering Law, Clamped Mode

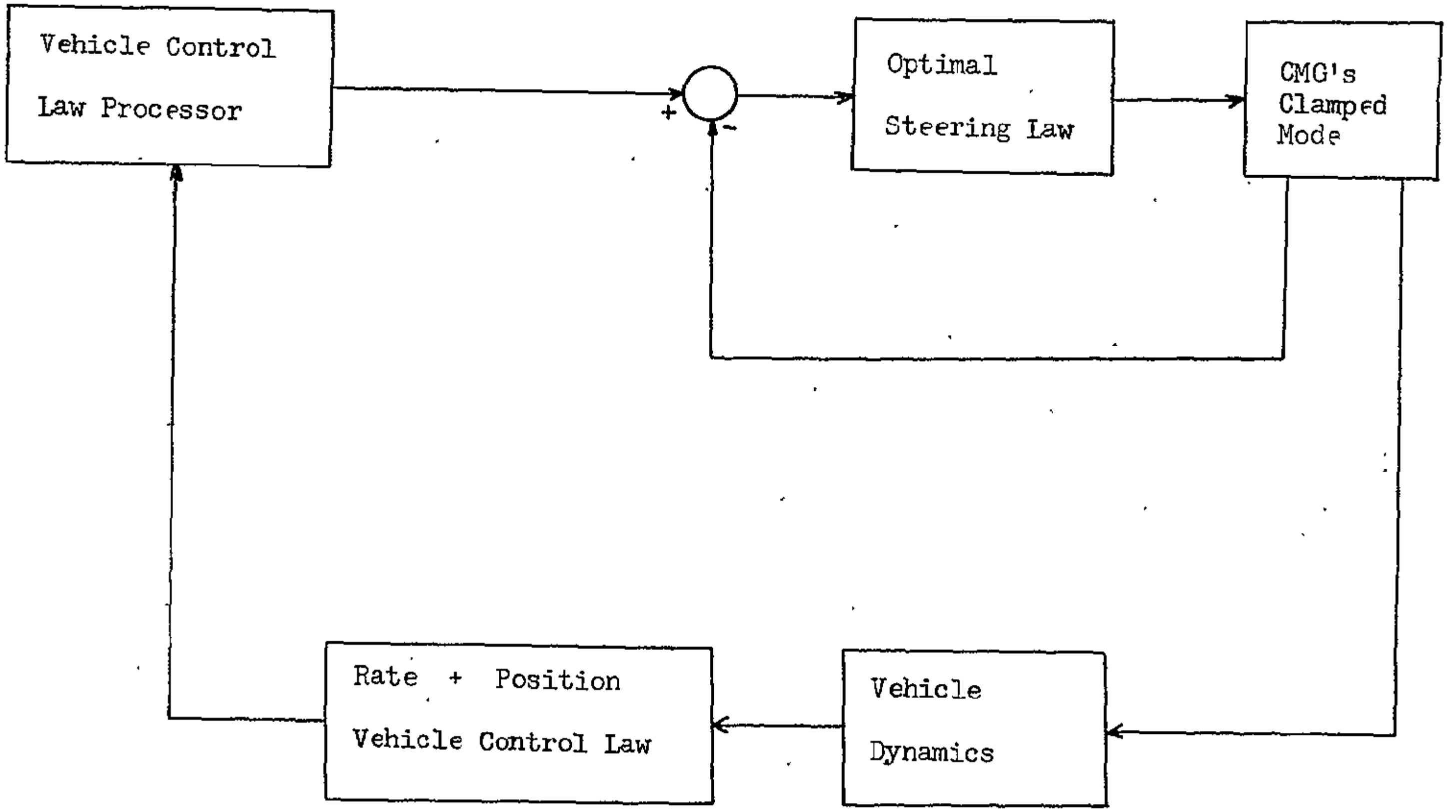

Figure 27. Single-Axis Block Diagram, Optimal Steering Law, Clamped Mode

together with the Optimal Steering Law, in order to provide the proper reaction moment on the vehicle.

Figures 28, 29, and 30 show the response of the x-axis of the system, the y-axis of the system, and the z-axis of the system due to an initial condition in the x-axis, the y-axis, and the z-axis, respectively.

System Comparison, Direct-Axis Response

As can be seen from Figures 20, 24, and 28, the response of the system with the CMG's in the clamped mode is superior to that of the system with the CMG's in the normal mode of operation. Also, the response of the system with the CMG's in the clamped mode using the Optimal Steering Law is better than the system response with the Cross-Product Steering Law.

Table 1 lists the rise time (time for output to go from 0 to 90% of final value), and the percent overshoot for each of the system configurations.

System Comparison, Cross-Axis Response

Figures 10 through 13 and 15 through 18 show that the design objective of minimizing the cross-axis response is virtually achieved using the Optimal Steering Law with the system configuration having the CMG's in the clamped mode of operation.

System Stability

This section presents the results of a study made in order to

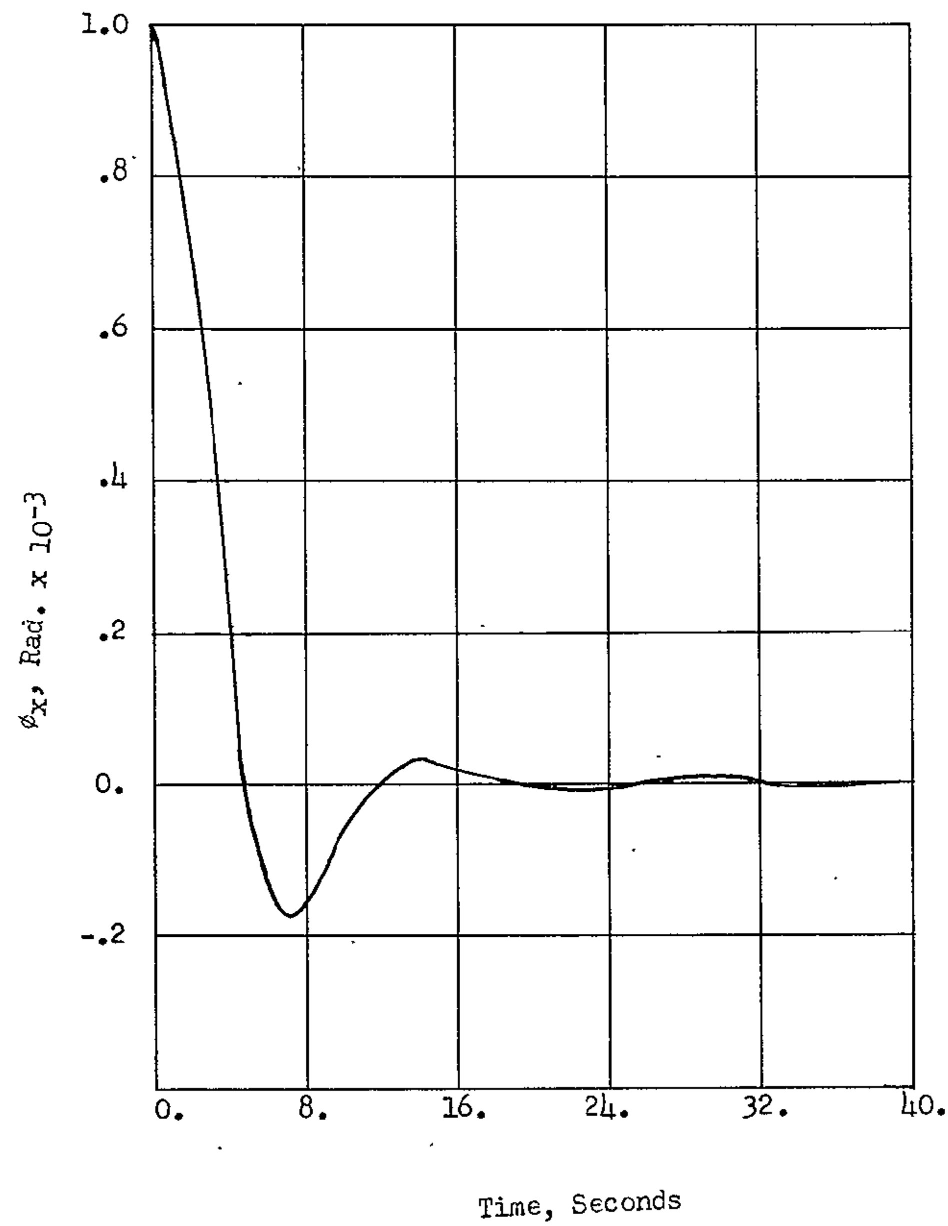

Figure 28. X-Axis Response, Optimal Steering Law, Clamped Mode

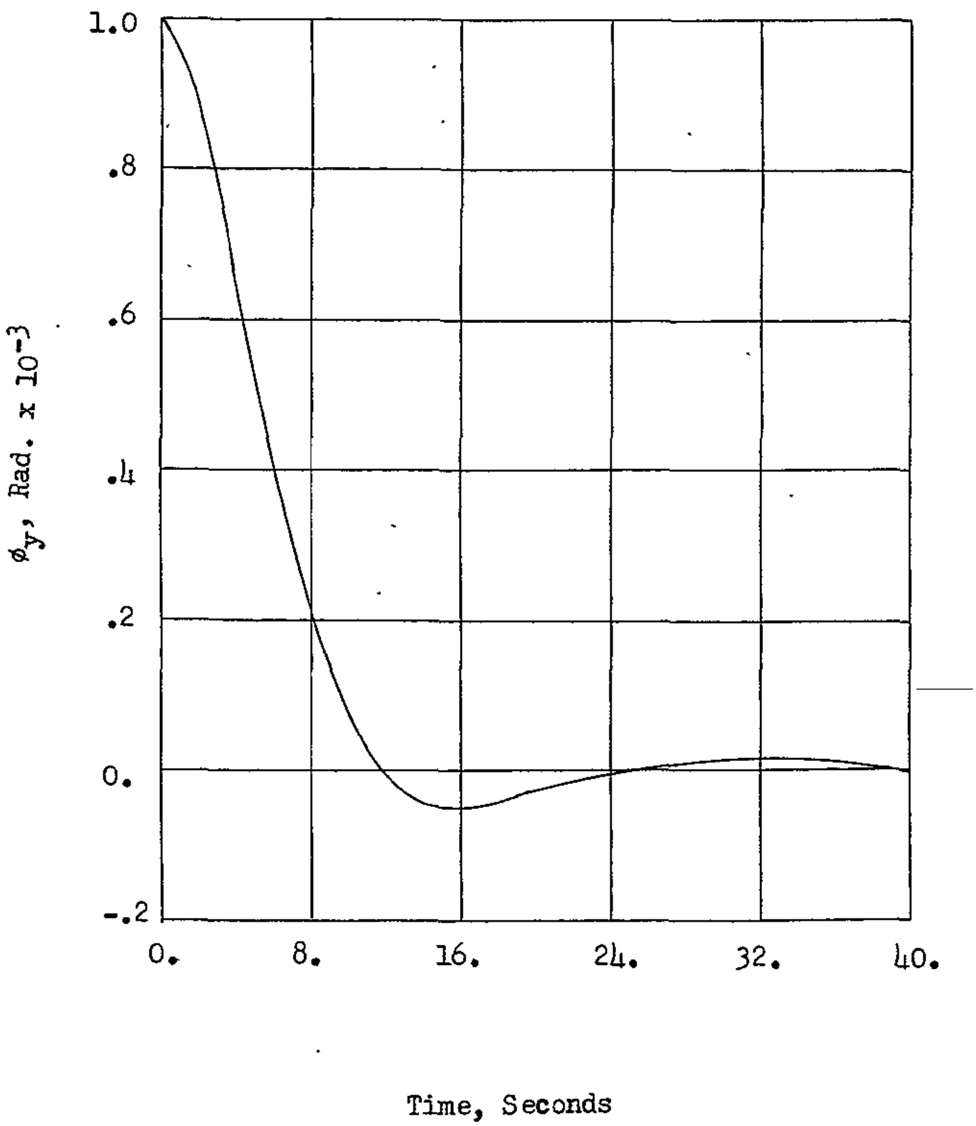

Figure 29. Y-Axis Response, Optimal Steering Law, Clamped Mode

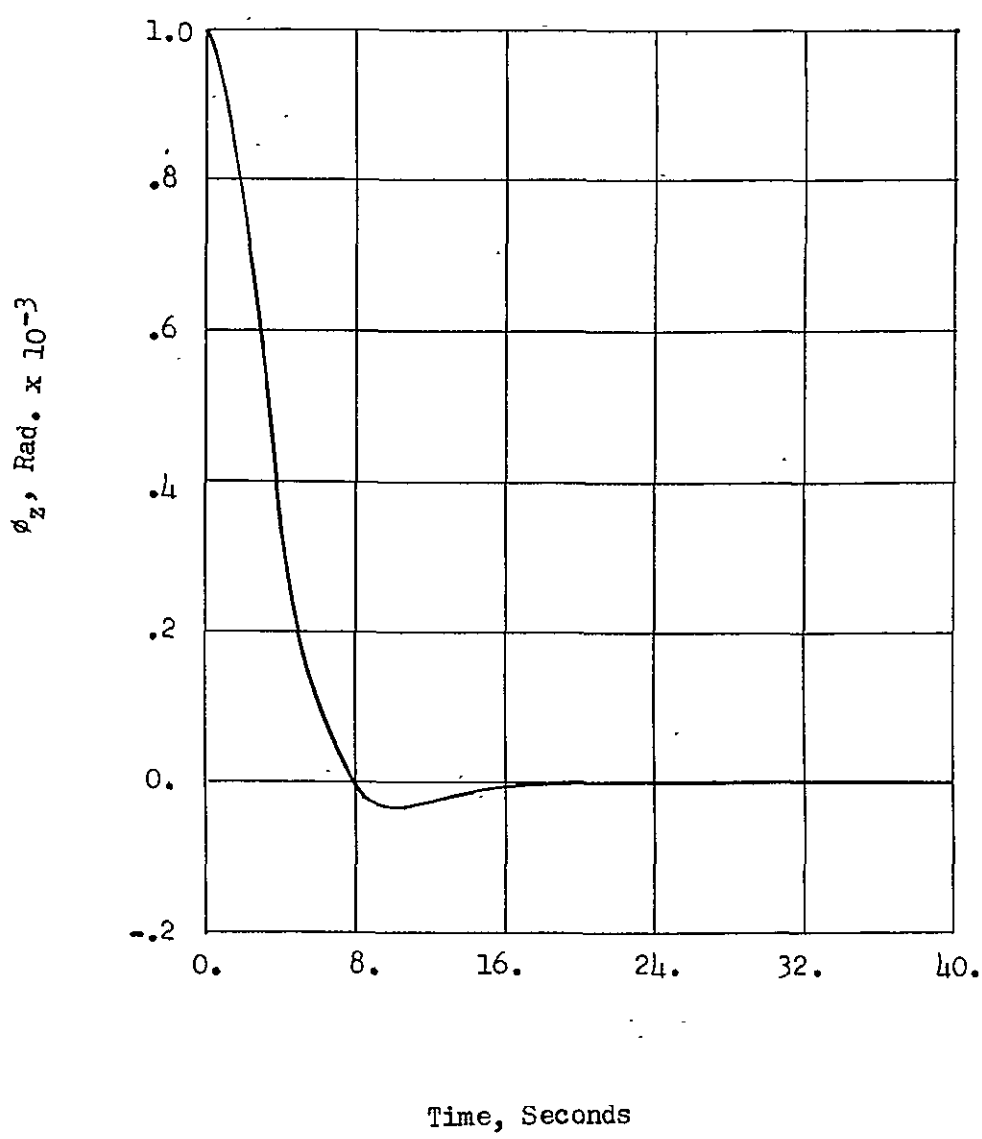

Figure 30. Z-Axis Response, Optimal Steering Law, Clamped Mode

	Optimal Steering Law Clamped Mode	Cross-Product Steering Law Clamped Mode	Cross-Product Steering Law Normal Mode
Rise Time	4.2 Sec.	4.5 Sec.	5.6 Sec.
% Overshoot	17.5%	28%	32%

Table 1. Rise Time and Percent Overshoot for Various System Configurations

$H_{xv} = 2.,\ H_{yv} = 1.,\ H_{zv} = 0.$

$\delta_{1(1)} = \delta_{1(2)} = \delta_{1(3)} = 0.$ deg.

$\delta_{3(1)} = -.05$ deg., $\delta_{3(2)} = 2.56$ deg., $\delta_{3(3)} = -87.4$ deg.

$H_{xv} = 0.,\ H_{yv} = 2.,\ H_{zv} = 1.$

$\delta_{1(1)} = \delta_{1(2)} = \delta_{1(3)} = 0.$ deg.

$\delta_{3(1)} = -87.44$ deg., $\delta_{3(2)} = -.06$ deg., $\delta_{3(3)} = 2.56$ deg.

Table 2. Two Outer Gimbal Location Criterion Solutions

0

determine the stability characteristics of the system with the CMG's in the clamped mode of operation.

Normal Mode, Cross-Product Steering Law

In order to have a basis for comparison, a stability study was performed on the system configuration with the Cross-Product Steering Law with the CMG's in the normal mode of operation. The region of stability for each axis was determined by finding the initial condition for which the system response became unstable. The value of initial condition for instability was found to be approximately .00275 rad. in the y-axis, and approximately .00125 rad. in the z-axis. The system was stable for initial conditions up to .003 rad. in the x-axis. No iniital conditions larger than .003 rad. were investigated.

Clamped Mode, Cross-Product Steering Law

The stability regions for the system configuration having the Cross-Product Steering Law with the CMG's in the clamped mode were determined from simulation studies. Results show that the system becomes unstable with an initial condition of approximately .00275 rad. on the x-axis, with an initial condition of approximately .00175 rad. on the y-axis and with an initial condition of approximately .00125 rad. on the z-axis.

Clamped Mode, Optimal Steering Law

As for the previous system configurations, the stability regions for the system having the Optimal Steering Law with the CMG's in the clamped mode of operation were determined from simulation studies. Results show that the system was stable with initial conditions up to .003 rad. on each axis. As stated previously, no initial conditions larger than .003 rad. were investigated.

System Comparison

From the results of the previous section, it can be seen that stability is not compromised by using the CMG's in the clamped mode of operation. The region of stability for the system comfiguration having the Cross-Product Steering Law with the CMG's in the normal mode is very similar to the region of stability for the system configuration having the Cross-Product Steering Law with the gyro's in the clamped mode. The region of stability for the system configuration having the Optimal Steering Law with the CMG's in the clamped mode is larger than for the two other system configurations investigated.

Location of the Outer Gimbals for Clamping

In order to clamp the outer gimbals at locations which provide maximum utilization of the system's capabilities, it is necessary to develop a criterion for use in selection of the locations at which the outer gimbal angles will be clamped.

The criterion selected is one which provides the maximum dynamic range, with regard to gimbal angle travel, for the inner gimbals during the clamped portion of the flight. However, for this criterion, there are possible momentum configurations for which this criterion cannot be satisfied. No work has been done in determining the probability that the momentum configuration would be such that the criterion could not be satisfied. A computer program has been developed which determines from a properly specified momentum configuration the locations at which the outer gimbals should be clamped in order to provide maximum dynamic range for the inner gimbals during the clamped portion of the flight. Table 2 (page 49) gives the values for two possible momentum configurations and the associated inner and outer gimbal locations which, for the given momentum configurations, satisfy the previously discussed criterion.

Saturation Characteristics Study

This section of the report presents the results of a study made in order to determine some of the dynamic characteristics of the system with regard to saturation by applying a small biased torque. An example of such a torque would be a gravity gradient torque. The results give an indication of the time that the system with the CMG's in the clamped mode would operate with a small disturbance torque before becoming saturated. Figures 31 and 32 show the plots of one of the gimbal angles versus time for a step disturbance torque on the x-axis. These plots are for the system configuration having the Cross-Product Steering Law with the CMG's in the clamped mode and for the system configuration having the Optimal Steering Law with the CMG's in the clamped mode, respectively.

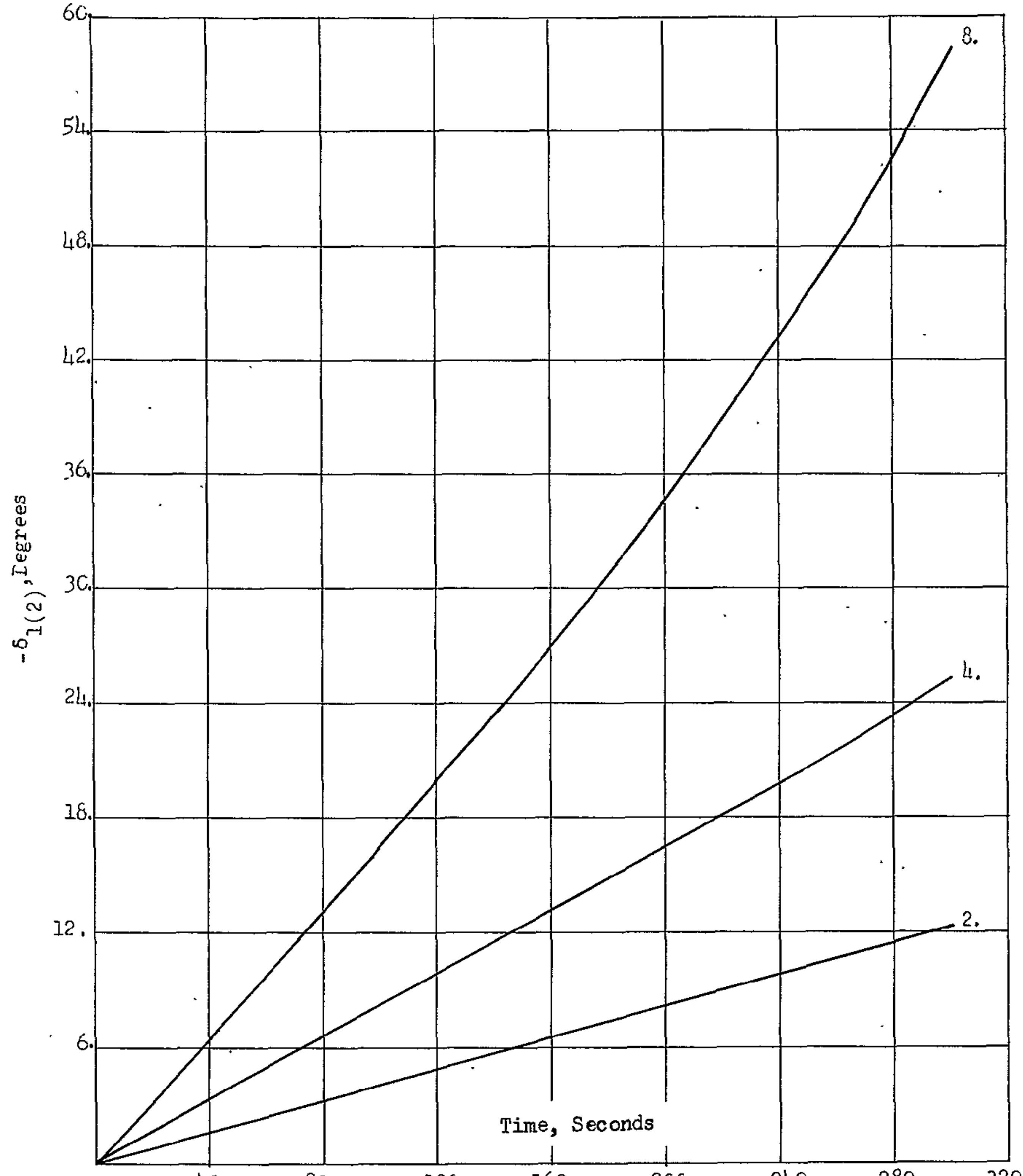

Figure 31. Gimbal Angle vs. Time, Cross-Product Steering Law, Clamped Mode

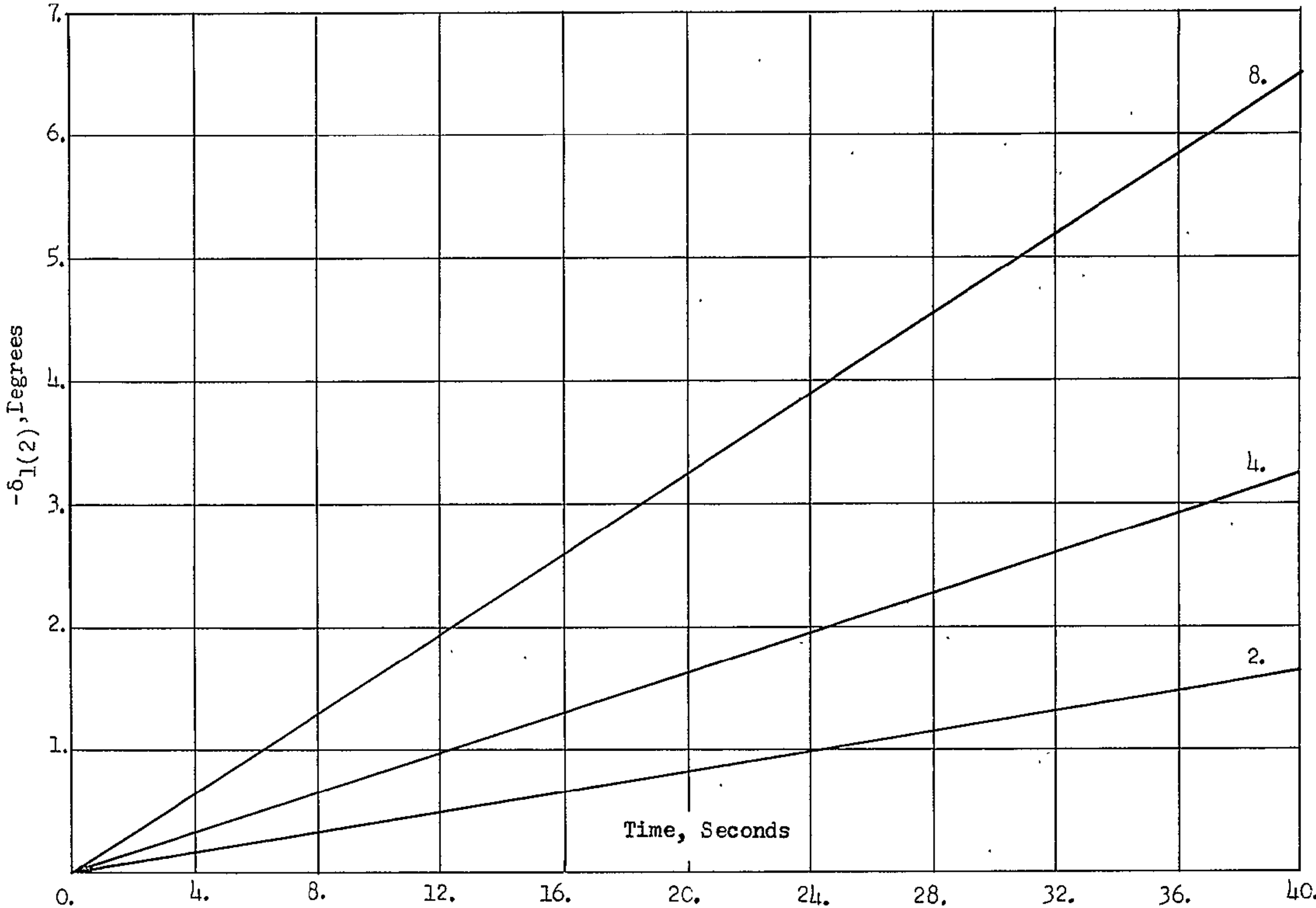

Figure 32. Gimbal Angle vs. Time, Optimal Steering Law, Clamped Mode

VI. CONCLUSIONS AND RECOMMENDATIONS

The results show that the bandwidth of the system is significantly increased by clamping the outer gimbals to the frame. This is exemplified by the amplitude-frequency characteristics in the frequency domain and the response curves in the time domain. The cross-axis response is greatly reduced by using the Optimal Steering Law with the system configuration having the outer gimbals clamped to the frame. The results show, therefore, that clamping the outer gimbals to the frame does provide a feasible approach for improving significantly the system characteristics. The clamping of the outer gimbals to the frame is also shown not to have an adverse effect on the system stability.

Additional studies should be made in order to provide a more complete investigation of the clamped mode of operation. Some of the areas which should be further investigated are (1) criterions for selection of the location of the outer gimbals during the clamped mode of operation, (2) the use of the H-vector control law for the inner CMG loop in conjunction with the Optimal Steering Law, and (3) the hardware requirements for implementation of the Optimal Steering Law.

REFERENCES

1. W. B. Chubb, D. N. Schultz and S. M. Seltzer, "Attitude control and precision pointing of the Apollo Telescope Mount," presented at the AIAA Guidance Control, and Flight Dynamics Conference, Huntsville, Alabama, August, 1967.

2. W. B. Chubb and Michael Epstein, "Application of control moment gyros in the attitude control of the Apollo Telescope Mount," presented at the AIAA Guidance, Control, and Flight Dynamics Conference, Pasadena, California, August, 1968.

3. M. T. Borelli, "An improved control system for the Apollo Telescope Mount," NASA TNX-53830, April, 1969.

APPENDIX A

Improved Attitude Control System Study Simulation Program, Optimal Steering Law, Clamped Mode

```
PARAM  CUTOFF =.05
PARAM  DEL31R=.7854,DEL32R=.7854,DEL33R=.7854
PARAM  INERTX=806900., INERTY=5243000., INERTZ=5090000.
INCON  PHIXIN=0.,PHIYIN=0.,PHIZIN=0.
INCON  PXDTIN=0.,PYDTIN=0.,PZDTIN=0.
       MXCMDE = MXCMND - MREX
       MYCMDE = MYCMND - MREY
       MZCMDE = MZCMND - MREZ
       MTRXD=COS(DEL31R)*SIN(DEL11R)*SIN(DEL12R)*COS(DEL32R)*...
       COS(DEL33R)*SIN(DEL13R) - (SIN(DEL31R)*SIN(DEL11R)...
       *SIN(DEL12R)*SIN(DEL32R)*SIN(DEL33R)*SIN(DEL13R)) + ...
       COS(DEL11R)*COS(DEL13R)*COS(DEL12R)  + COS(DEL11R)...
       *SIN(DEL12R)*COS(DEL32R)*SIN(DEL33R)*SIN(DEL13R) + ...
       SIN(DEL12R)*SIN(DEL32R)*COS(DEL13R)*COS(DEL31R)*SIN(DEL11R)+...
        COS(DEL33R)*SIN(DEL13R)*COS(DEL12R)*SIN(DEL31R)*SIN(DEL11R)
NOSORT
       IF(MTRXD.GE.0.) GO TO 2
    1  IF((MTRXD + CUTOFF) .LE. 0.) GO TO 3
       MTRXD = -CUTOFF
       GO TO 3
    2  CONTINUE
       IF((MTRXD - CUTOFF) .GE. 0.) GO TO 3
       MTRXD = CUTOFF
SORT
    3  DDT11C = ((SIN(DEL12R)*COS(DEL32R)*COS(DEL33R)*SIN(DEL13R)+...
       SIN(DEL12R)*SIN(DEL32R)*COS(DEL13R))*MXCMDE + (SIN(DEL12R)*...
       SIN(DEL32R)*SIN(DEL33R)*SIN(DEL13R) - COS(DEL12R)*COS(DEL33R)*...
       SIN(DEL13R))*MYCMDE + (COS(DEL12R)*COS(DEL13R) + SIN(DEL12R)*...
       COS(DEL32R)*SIN(DEL33R)*SIN(DEL13R))*MZCMDE)/(MTRXD * 2820.)
       DDT12C = ((SIN(DEL31R)*SIN(DEL11R)*COS(DEL33R)*SIN(DEL13R) + ...
       COS(DEL11R)*COS(DEL13R))*MXCMDE+ (COS(DEL31R)*SIN(DEL11R)*...
       COS(DEL33R)*SIN(DEL13R) + COS(DEL11R)*SIN(DEL33R)*...
       SIN(DEL13R))*MYCMDE + (SIN(DEL31R)*SIN(DEL11R)*SIN(DEL33R)*...
       SIN(DEL13R) - COS(DEL31R)*SIN(DEL11R)*COS(DEL13R))*...
       MZCMDE)/(MTRXD*2820.)
       DDT13C = ((SIN(DEL31R)*SIN(DEL11R)*SIN(DEL12R)*SIN(DEL32R) -...
       COS(DEL11R)*SIN(DEL12R)*COS(DEL32R))*MXCMDE + (COS(DEL31R)*...
       SIN(DEL11R)*SIN(DEL12R)*SIN(DEL32R) + COS(DEL11R)*COS(DEL12R))*...
       MYCMDE +(COS(DEL31R)*SIN(DEL11R)*SIN(DEL12R)*COS(DEL32R) +...
       SIN(DEL31R)*SIN(DEL11R)*COS(DEL12R))*MZCMDE)/(MTRXD*2820.)
       DDT11G = 2.*DDT11C
       M1 = DDT11G - 5.*M1INT
       M1INT = INTGRL(0.,M1)
       DDT11R= 5.*M1INT
       DDT12G = 2.*DDT12C
       M2 = DDT12G - 5.*M2INT
       M2INT = INTGRL(0.,M2)
       DDT12R= 5.*M2INT
       DDT13G = 2.*DDT13C
       M3 = DDT13G - 5.*M3INT
       M3INT = INTGRL(0.,M3)
       DDT13R= 5.*M3INT
       DEL11R= INTGRL(0.0,DDT11R)
       DEL12R= INTGRL(0.0,DDT12R)
       DEL13R= INTGRL(0.0,DDT13R)
       MRX = (COS(DEL31R)*SIN(DEL11R)*DDT11R + COS(DEL12R)*DDT12R -...
       SIN(DEL32R)*SIN(DEL13R)*DDT13R)*2820.
       MRY = (-SIN(DEL31R)*SIN(DEL11R)*DDT11R + COS(DEL32R)*...
       SIN(DEL12R)*DDT12R + COS(DEL13R)*DDT13R)*2820.
       MRZ = (COS(DEL11R)*DDT11R  - SIN(DEL32R)*SIN(DEL12R)*DDT12R+...
```

NOT REPRODUCIBLE

```
      COS(DEL33R)*SIN(DEL13R)*DDT13R)*2820.
      MRXD = MRX + 4.
      TRXV =  MRXD/INERTX
      TRYV= MRY /INERTY
      TRZV= MRZ /INERTZ
      PHIX = INTGRL(PHIXIN,PHIXDT)
      PHIXDT=INTGRL(PXDTIN,TRXV)
      PHIY = INTGRL(PHIYIN,PHIYDT)
      PHIYDT=INTGRL(PYDTIN,TRYV)
      PHIZ = INTGRL(PHIZIN,PHIZDT)
      PHIZDT=INTGRL(PZDTIN,TRZV)
      MXCMND=-(200000.*PHIX + 400000.*PHIXDT)
      MYCMND=-(400000.*PHIY + 2000000.*PHIYDT)
      MZCMND=-(1000000.*PHIZ + 3330000.*PHIZDT)
      DEL11= DEL11R*57.29578
      DEL12= DEL12R*57.29578
      DEL13= DEL13R*57.29578
      DLDT11=DDT11R*57.29578
      DLDT12=DDT12R*57.29578
      DLDT13=DDT13R*57.29578
PRINT DEL11,DEL12,DEL13,DLDT11,DLDT12,DLDT13,MXCMND,MXCMDE,MRX,...
      MRY,MRZ,MTRXD,PHIX,PHIY,PHIZ,DDT11C,DDT12C,DDT13C
TIMER FINTIM=40.,DELT=.02,PRDEL=.10,OUTDEL=.10
FINISH DEL11R=2.,DEL12R=2.,DEL13R=2.
METHOD RKSFX
      END
      STOP
ENDJOB
```

APPENDIX B

Improved Attitude Control System Study Simulation Program, Cross-Product Steering Law, Clamped Mode

```
PARAM  DEL31R=.7854,DEL32R=.7854,DEL33R=.7854
PARAM  INERTX=826500.,  INERTY=5243000.,  INERTZ=5050000.
INCON  PXDTIN=0.,PYDTIN=0.,PZDTIN=0.
INCON  PHIXIN=0.,PHIYIN=0.,PHIZIN=0.
       HXCMND = INTGRL(0.,TXC)
       HYCMND = INTGRL(0.,TYC)
       HZCMND = INTGRL(0.,TZC)
       HXCMDL = LIMIT(-8460.,8460.,HXCMND)
       HYCMDL = LIMIT(-8460.,8460.,HYCMND)
       HZCMDL = LIMIT(-8460.,8460.,HZCMND)
       HXCMDE = HXCMDL - HXV
       HYCMDE = HYCMDL - HYV
       HZCMDE = HZCMDL - HZV
       HXCDEL = LIMIT(-140.,140.,HXCMDE)
       HYCDEL = LIMIT(-140.,140.,HYCMDE)
       HZCDEL = LIMIT(-140.,140.,HZCMDE)
       DDT11C= .0005808*((-COS(DEL31R)*SIN(DEL11R)*HXCDEL)+...
       (SIN(DEL31R)*SIN(DEL11R)*HYCDEL)+ (-COS(DEL11R)* HZCDEL))
       DDT12C=.0005808*((-COS(DEL12R)*HXCDEL)+ (-COS(DEL32R)*...
       SIN(DEL12R)*HYCDEL)+(SIN(DEL32R)*SIN(DEL12R)*HZCDEL))
       DDT13C=.0005808*((SIN(DEL33R)*SIN(DEL13R)* HXCDEL)+...
       (-COS(DEL13R)*HYCDEL)+(-COS(DEL33R)*SIN(DEL13R)*HZCDEL))
       DDT11R = DDT11C
       DDT12R = DDT12C
       DDT13R = DDT13C
       DEL11R= INTGRL(0.0,DDT11R)
       DEL12R= INTGRL(0.0,DDT12R)
       DEL13R= INTGRL(0.0,DDT13R)
       HXV= 2920.*(COS(DEL31R)*COS(DEL11R)-SIN(DEL12R)-...
       SIN(DEL33R)* COS(DEL13R))
       HYV= 2920.*(-SIN(DEL31R)*COS(DEL11R)+COS(DEL32R)*COS(DEL12R)
       SIN(DEL13R))
       HZV= 2920.*(-SIN(DEL11R)-SIN(DEL32R)*COS(DEL12R)+...
       COS(DEL33R)*COS(DEL13R))
       MRX = (COS(DEL31R)*SIN(DEL11R)*DDT11R + COS(DEL12R)*DDT12R -
       SIN(DEL33R)*SIN(DEL13R)*DDT13R)*2920.
       MRY = (-SIN(DEL31R)*SIN(DEL11R)*DDT11R + COS(DEL32R)*...
       SIN(DEL12R)*DDT12R + COS(DEL13R)*DDT13R)*2920.
       MRZ = (COS(DEL11R)*DDT11R  - SIN(DEL32R)*SIN(DEL12R)*DDT12R+
       COS(DEL33R)*SIN(DEL13R)*DDT13R)*2920.
       DEL11= DEL11R*57.29578
       DEL12= DEL12R*57.29578
       DEL13= DEL13R*57.29578
       DLDT11=DDT11R*57.29578
       DLDT12=DDT12R*57.29578
        DLDT13=DDT13R*57.29578
       DEL31=DEL31R*57.29578
       DEL32=DEL32R*57.29578
       DEL33=DEL33R*57.29578
       HYC = -HYV
       HZC = -HZV
       MRXD = MRX + 4.
       TRXV = -MRXD/INERTX
       TRYV=-MRY /INERTY
       TRZV=-MRZ /INERTZ
       PHIXDT=INTGRL(PXDTIN,TRXV)
       PHIX = INTGRL(PHIXIN,PHIXDT)
       PHIYDT=INTGRL(PYDTIN,TRYV)
       PHIY =INTGRL(PHIYIN,PHIYDT)
       PHIZDT=INTGRL(PZDTIN,TRZV)
```

NOT REPRODUCIBLE

```
        PHIZ = INTGRL(PHIZIN,PHIZDT)
        TXC = -(200000.*PHIX + 400000.*PHIXDT)
        TYC = -(400000.*PHIY + 2000000.*PHIYDT)
        TZC=-(400000.*PHIZ + 1320000.*PHIZDT)
PRINT   TXC,HXCMDL,HXV,HYC,HZC,DEL11,DEL12,DEL13,PHIX,PHIY,PHIZ,...
        HXCDEL,MDX,MDY,MDZ,DDT11C,DDT12C,DDT13C
TIMER  FINTIM=300.,DELT=.5,PRDEL=.5,OUTDEL=.5
FINISH DEL11P=2.,DEL12P=2.,DEL13P=2.
METHOD RKSFX
        END
         STOP
ENDJOB
```

APPENDIX C

Improved Attitude Control System Study Simulation Program, Cross-Product Steering Law, Normal Mode

```
PARAM  INERTX=8069C0., INERTY=5243CCC., INERTZ=5090000.
INCON  PHIXIN=C.,PHIYIN=.0025,PHIZIN=.0
INCON  PXDTIN=C.,PYDTIN=C.,PZDTIN=0.
       HXCMND = INTGRL(0.,TXC)
       HYCMND = INTGRL(0.,TYC)
       HZCMND = INTGRL(0.,TZC)
       HXCMDL = LIMIT(-8460.,8460.,HXCMND)
       HYCMDL = LIMIT(-8460.,8460.,HYCMND)
       HZCMDL = LIMIT(-8460.,8460.,HZCMND)
       HXCMDE = HXCMDL - HXV
       HYCMDE = HYCMDL - HYV
       HZCMDE = HZCMDL - HZV
       HXCDEL = LIMIT(-140.,140.,HXCMDE)
       HYCDEL = LIMIT(-140.,140.,HYCMDE)
       HZCDEL = LIMIT(-140.,140.,HZCMDE)
       DDT11C= .0005808*((-COS(DEL31R)*SIN(DEL11R)*HXCDEL)+...
       (SIN(DEL31R)*SIN(DEL11R)*HYCDEL)+ (-COS(DEL11R)* HZCDEL))
       DDT12C=.0005805*((-COS(DEL12R)*HXCDEL)+ (-COS(DEL32R)*...
       SIN(DEL12R)*HYCDEL)+(SIN(DEL32R)*SIN(DEL12R)*HZCDEL))
       DDT13C=.0005808*((SIN(DEL33R)*SIN(DEL13R)* HXCDEL)+...
       (-COS(DEL13R)*HYCDEL)+(-COS(DEL33R)*SIN(DEL13R)*HZCDEL))
       DDT31C=.0005808*((-SIN(DEL31R)*HXCDEL)+ (-COS(DEL31R)*HYCDEL))
       DDT32C= .0005808*((-SIN(DEL32R)*HYCDEL)+ (-COS(DEL32R)*HZCDEL))
       DDT33C=.0005808*((-COS(DEL33R)*HXCDEL)+(-SIN(DEL33R)*HZCDEL))
       DDT11R = DDT11C
       DDT12R = DDT12C
       DDT13R = DDT13C
       DDT31R = DDT31C
       DDT32R = DDT32C
       DDT33R = DDT33C
       DEL11R= INTGRL(0.0,DDT11R)
       DEL12R= INTGRL(0.0,DDT12R)
       DEL13R= INTGRL(0.0,DDT13R)
       DEL31R = INTGRL(.7854,DDT31R)
       DEL32R = INTGRL(.7854,DDT32R)
       DEL33R = INTGRL(.7854,DDT33R)
       HXV= 2820.*(COS(DEL31R)*COS(DEL11R)-SIN(DEL12R)-...
       SIN(DEL33R)* COS(DEL13R))
       HYV= 2820.*(-SIN(DEL31R)*COS(DEL11R)+COS(DEL32R)*COS(DEL12R)-...
       SIN(DEL13R))
       HZV= 2820.*(-SIN(DEL11R)-SIN(DEL32R)*COS(DEL12R)+...
       COS(DEL33R)*COS(DEL13R))
       MRX = (COS(DEL31R)*SIN(DEL11R)*DDT11R + COS(DEL12R)*DDT12R -...
       SIN(DEL33R)*SIN(DEL13R)*DDT13R)*2820.
       MRY = (-SIN(DEL31R)*SIN(DEL11R)*DDT11R + COS(DEL32R)*...
       SIN(DEL12R)*DDT12R + COS(DEL13R)*DDT13R)*2820.
       MRZ = (COS(DEL11R)*DDT11R  - SIN(DEL32R)*SIN(DEL12R)*DDT12R+...
       COS(DEL33R)*SIN(DEL13R)*DDT13R)*2820.
       DEL11= DEL11R*57.29578
       DEL12= DEL12R*57.29578
       DEL13= DEL13R*57.29578
       DLDT11=DDT11R*57.29578
       DLDT12=DDT12R*57.29578
        DLDT13=DDT13R*57.29578
       DEL31=DEL31R*57.29578
       DEL32=DEL32R*57.29578
       DEL33=DEL33R*57.29578
       HYE = -HYV
       HZE = -HZV
       TRXV=-MRX /INERTX
```

```
      TRYV=-MRY /INERTY
      TRZV=-MRZ /INERTZ
      PHIXDT=INTGRL(PXDTIN,TRXV)
      PHIX = INTGRL(PHIXIN,PHIXDT)
      PHIYDT=INTGRL(PYDTIN,TRYV)
      PHIY = INTGRL(PHIYIN,PHIYDT)
      PHIZDT=INTGRL(PZDTIN,TRZV)
      PHIZ = INTGRL(PHIZIN,PHIZDT)
      TXC = -(200000.*PHIX + 400000.*PHIXDT)
      TYC = -(400000.*PHIY + 2000000.*PHIYDT)
      TZC = -(1000000.*PHIZ + 3330000.*PHIZDT)
PRINT  TXC,HXCMDL,HXV,HYE,HZE,DEL11,DEL12,DEL13,DEL31,DEL32,DEL33,...
      HXCDEL,MRX,MRY,MRZ,PHIX,PHIY,PHIZ,DDT11C,DDT12C,DDT13C
PRTPLT TXC,HXCMDL,HXV,HYE,HZE,DEL11,DEL12,DEL13,DEL31,DEL32,DEL33,HXCDEL
PRTPLT MRX,MRY,MRZ,PHIX,PHIY,PHIZ
TIMER FINTIM=60.,DELT=.5,PRDEL=.5,OUTDEL=.5
FINISH DEL11R=2.,DEL12R=2.,DEL13R=2.
METHOD RKSFX
      END
       STOP
ENDJOB
```

APPENDIX D

Outer Gimbal Angle Criterion Solution Program

```
C   A BLANK CARD IS NECESSARY TO END THE DATA
  1   READ(5,2) HXV,HYV,HZV
      IF(HXV.EQ.0..AND.HYV.EQ.0..AND.HZV.EQ.0.) GO TO 100
      B = .0001
      WRITE (6,11)
      WRITE(6,6)
      WRITE(6,4) HXV,HYV,HZV,B
      DEL31W = .7854
      DEL32W = .7854
      DEL33W = .7854
      I = 1
  3   DEL31=DEL31W
      DEL32=DEL32W
      DEL33=DEL33W
      HNO31=(COS(DEL32W)-HYV)/(HXV + SIN(DEL33W))
      DEL31W=ATAN(HNO31)
      HNO32=(COS(DEL33W)-HZV)/(HYV + SIN(DEL31W))
      DEL32W=ATAN(HNO32)
      HNO33=(COS(DEL31W)-HXV)/(HZV + SIN(DEL32W))
      DEL33W=ATAN(HNO33)
      HXVC = COS(DEL31W) - SIN(DEL33W)
      HYVC = COS(DEL32W) - SIN(DEL31W)
      HZVC = COS(DEL33W) - SIN(DEL32W)
      TEST1 = ABS(HXV - HXVC)
      TEST2 = ABS(HYV - HYVC)
      TEST3 = ABS(HZV - HZVC)
      IF(TEST1.LE.B.AND.TEST2.LE.B.AND.TEST3.LE.B) GO TO 10
      IF(I.EQ.1000) GO TO 60
      I = I + 1
  5   GO TO 3
 60   WRITE(6,26)
      WRITE(6,25)
      WRITE(6,26)
 10   CONTINUE
      DEL31=57.29578*DEL31W
      DEL32=57.29578*DEL32W
      DEL33=57.29578*DEL33W
      WRITE (6,22)
      WRITE(6,15) DEL31,DEL32,DEL33
      HXVC= COS(DEL31W) - SIN(DEL33W)
      HYVC= COS(DEL32W) - SIN(DEL31W)
      HZVC=COS(DEL33W) - SIN(DEL32W)
      WRITE(6,20)
      WRITE(6,21) HXVC,HYVC,HZVC
      GO TO 1
  2   FORMAT(4F10.4)
  6   FORMAT(//,20X,21HTHE INITIAL MOMENTUM VALUES ARE)
  4   FORMAT(//,15X,7H HXVI= ,F10.4,10X,7H HYVI= ,F10.4,10X,7H HZVI=
     10.4,5X,16HACCURACY SPEC.= ,F8.6)
 11   FORMAT(1H1)
 15   FORMAT(//,15X,7HDEL31= ,F8.4,8H DEGREES,10X,7HDEL32= ,F8.4,8H D
     JEES,10X,7HDEL33= ,F8.4,8H DEGREES)
 20   FORMAT(//,20X,47HTHESE ANGLES GIVE THE FOLLOWING MOMENTUM VALUE
 21   FORMAT(15X,6H HXV= ,F10.4,10X,6H HYV= ,F10.4,10X,6H HZV= ,F10.4
 22   FORMAT(//,15X,25HTHE CALCULATED ANGLES ARE)
 25   FORMAT(//,40X,40HFAILED TO CONVERGE AFTER 1000 ITERATIONS)
 26   FORMAT(//,40X,40H****************************************)
100   STOP
```